Title

Salmonella persisters promote the spread of antibiotic resistance plasmids in the gut.

Journal

Nature: New biology, 573(7773)

Authors

Bakkeren, Erik

Huisman, Jana

Fattinger, Stefan

et al.

Publication Date

2019-09-01

DOI

10.1038/s41586-019-1521-8

Peer reviewed

Published in final edited form as:
Nature. 2019 August 10; 573(7773): 276–280. doi:10.1038/s41586-019-1521-8.

Salmonella persisters promote the spread of antibiotic resistance plasmids in the gut

Erik Bakkeren[1], **Jana S. Huisman**[2,3], **Stefan A. Fattinger**[1,4], **Annika Hausmann**[1], **Markus Furter**[1], **Adrian Egli**[5,6], **Emma Slack**[1,7], **Mikael E. Sellin**[4], **Sebastian Bonhoeffer**[2], **Roland R. Regoes**[2], **Médéric Diard**[#1,8,*], **Wolf-Dietrich Hardt**[#1,*]

[1]Institute of Microbiology, Department of Biology, ETH Zurich, Zurich, Switzerland [2]Institute of Integrative Biology, Department of Environmental Systems Science, ETH Zurich, Zurich, Switzerland [3]Swiss Institute of Bioinformatics, Lausanne, Switzerland [4]Science for Life Laboratory, Department of Medical Biochemistry and Microbiology, Uppsala University, Uppsala, Sweden [5]Division of Clinical Microbiology, University Hospital Basel, Basel, Switzerland [6]Applied Microbiology Research, Department of Biomedicine, University of Basel, Basel, Switzerland [7]Institute of Food, Nutrition and Health, Department of Health Sciences and Technology, ETH Zurich, Zurich, Switzerland [8]Biozentrum, University of Basel, Basel, Switzerland

[#] These authors contributed equally to this work.

Summary

The emergence of antibiotic resistant bacteria by mutations or by acquisition of genetic material like resistance plasmids represents a major public health issue [1,2] (Extended Data Fig. 1a). Persisters are bacterial subpopulations surviving antibiotics by reversibly adapting their

[*]**Corresponding authors**: Correspondence should be addressed to Médéric Diard (mederic.diard@unibas.ch) or Wolf-Dietrich Hardt (wolf-dietrich.hardt@micro.biol.ethz.ch).

Data availability statement:
The genome and plasmid sequence of *E. coli* ESBL 15 were deposited in GenBank under accession numbers CP041678-CP041681 (Biosample SAMN12275742). Numerical source data for all figures are provided with the paper. Source images are available upon request to the corresponding authors.

Code availability statement:
Code for the stochastic simulation of plasmid transfer dynamics and parameter estimation from the experimental data is provided with the paper. All R-code needed to simulate the stochastic model, estimate the most likely parameters from the experimental data, and plot the results, is included in a zip-folder.

Ethical statement:
All animal experiments were ethically approved by the responsible authorities (Tierversuchskommission, Kantonales Veterinäramt Zürich, license 193/2016). In four cases, data from mice were excluded since the animals needed to be sacrificed prematurely due to disease or symptom severity.

Contributions:
EB (figures 1, 2, 3a-b, 3e-f, 4, ED1-3, ED4a-c, e-f, ED5-9), SAF (figures 1E, ED4a-d), AH (figures 2, ED5, ED6e-f, ED9e), MF (figure ED4e-h), ES (figures 3E-F, ED7b) performed the experiments. JSH, SB and RRR (figures 3C-D, ED1b, ED6g, ED10) performed mathematical modeling. AE (figure ED1b) provided *E. coli* strain Z2115. EB, MD and WDH designed the experiments. SAF, MF, and MES designed the microscopy-based experiments and analysis. EB, MD, and WDH conceived the project and wrote the manuscript. All authors read, commented, and approved this manuscript.

Competing interests
The authors declare no competing financial interests.

Europe PMC Funders Author Manuscripts

physiology [3–10]. They promote the emergence of antibiotic resistant mutants [11]. We asked if persisters can also promote the spread of resistance plasmids. In contrast to mutations, resistance plasmid transfer requires the co-occurrence of two different bacterial strains: a donor and a recipient (Extended Data Fig. 1a). For our experiments, we chose the facultative intracellular entero-pathogen *Salmonella enterica* serovar Typhimurium (*S.*Tm) and *E. coli*, a common microbiota member [12]. *S.*Tm forms persisters surviving antibiotic therapy in several host tissues. We show that tissue-associated, *S.*Tm persisters account for long-lived reservoirs of plasmid donors or recipients. Persistent *S.*Tm reservoir formation requires *Salmonella* Pathogenicity Island (SPI) -1/2 in the gut-associated tissues or SPI-2 at systemic sites. Re-seeding of these bacteria into the gut lumen allows co-occurrence of donors with gut-resident recipients, thereby favouring plasmid transfer between various Enterobacteriaceae. We observe up to 99% transconjugants within 2-3 days after re-seeding. Mathematical modeling shows that rare re-seeding events may suffice for a high frequency of conjugation. Vaccination reduces tolerant reservoir formation after oral *Salmonella* infection and subsequent plasmid transfer. We conclude that even without selection for plasmid-encoded resistance genes, small persistent pathogen reservoirs can foster the spread of promiscuous resistance plasmids in the gut.

Salmonella enterica and *E. coli* strains harbor numerous resistance plasmids [13,14] and different strains frequently colonize the same host [15–19]. High cell densities in the gut lumen allows high rates of plasmid transfer within and between species [20–22]. *S.*Tm strains can colonize the gut lumen and survive within tissues of the host for prolonged periods of time [5–7,15–17,23]. In the absence of suitable resistance genes, the gut luminal *S.*Tm population is eliminated by antibiotics within a few hours, while tissue-associated *S.*Tm persister cells survive >10 days [5–8,24] (supplementary discussion A). After antibiotic withdrawal, surviving cells can migrate to the gut lumen and resume growth [24]. We hypothesized that this promotes co-occurrence of donors with gut-luminal recipients and thereby fuels resistance plasmid transfer *in vivo*.

Wild-type *S.*Tm SL1344, which naturally carries P2, served as the donor. P2 is a well-characterized conjugative plasmid in Enterobacteriaceae [20–22] of the IncI1 incompatibility group (Extended Data Fig. 1b) [25]. We labeled P2 with a chloramphenicol resistance marker (P2^{cat}) to monitor plasmid transfer by plating (Extended Data Fig. 1c-d). Controls excluded cross-resistance for any resistance markers used in this study (Extended Data Fig. 2). In the "oral model", the donor (*S.*Tm P2^{cat}) initially colonized the gut lumen and invaded host tissues (Fig. 1a-b; Extended Data Fig. 3). Ciprofloxacin cleared the gut luminal bacteria, while tissue-associated *S.*Tm P2^{cat} persisters survived [5–8]. The recipient *S.*Tm ATCC 14028S (naturally lacking P2) was introduced at day 8 [21,22]. Transconjugants (recipients that obtained the plasmid) replaced the recipients within 1-3 days after donor re-seeding (>99% median; day 11-12 of experiment; Fig. 1C; Extended Data Fig. 3a). Control experiments refuted that the rise of the transconjugants is attributable to P2-mediated fitness benefits over the recipients (Extended Data Fig. 3d-e). Further controls verified that P2^{cat} transfer occurs in the gut lumen (Extended Data Fig. 3f-g) and that P2^{cat} spreads by conjugation (Extended Data Fig. 3h-i). Non-invasive donor mutants (*S.*Tm^{noninv} P2^{cat}) indicated that donor cells originated from persistent tissue-associated *S.*Tm P2^{cat} reservoirs (Fig. 1c-e; Extended Data

Fig. 3b, 4). However, this cannot definitively rule out that rare persisters could also exist in the gut lumen.

To verify the importance of tissue-associated, persistent *S.*Tm reservoirs we employed an intravenous infection model (I.V. model; Fig. 2a-b). In line with previous work [23], *S.*Tm P2^{cat} formed large populations of persisters surviving intraperitoneal ceftriaxone treatment in the spleen and the liver (Fig. 2c-d; Extended Data Fig. 5a). In contrast to the oral model, gut luminal colonization by *S.*Tm P2^{cat} is observed only very rarely by day 5 (Extended Data Fig. 5). Nevertheless, when donors were detected in the gut lumen, transconjugants were formed with high efficiency within 1-3 days (Fig. 2e; Extended Data Fig. 5b). Donors lacking a key virulence factor promoting systemic pathogen growth *in vivo* [26] and the survival of persisters [27](*S.*Tm^{SPI-2} P2^{cat}), yielded much smaller persister reservoirs than wild type *S.*Tm P2^{cat} (Fig. 2d) and failed to produce transconjugants (Fig. 2e; Extended Data Fig. 5c). We conclude that tissue-associated *S.*Tm persisters can serve as reservoirs promoting the spread of conjugative plasmids.

Next, we identified the rate-limiting process in transconjugant formation *in vivo*, focusing on the oral model. Three key parameters may dictate plasmid transfer dynamics: 1) re-seeding, i.e. the rate at which plasmid-carrying donors re-enter the gut lumen and perform the initial conjugation event (dependent on the persistent reservoir population), 2) the rate of plasmid transfer from transconjugants to recipients, and 3) the relative growth rate of transconjugants over recipients. To estimate these rates, we used donor-mixtures carrying five DNA-tagged P2^{cat} variants (*S.*Tm P2$^{cat\ TAG}$; Extended Data Fig. 6). While all tags were present at roughly equivalent abundance in the inoculum, the feces (day 1) and the mucosa (day 15), most transconjugant populations harbored just one or two of the five tags (Fig. 3a-b; Extended Data Fig. 6b-c). In the I.V. infection experimental setup (Fig. 2b, 2e), transconjugants were also dominated by only one tag (Extended Data Fig. 6d-f). Thus, transconjugant populations arise from very few donor-to-recipient conjugation events, followed by transconjugant-to-recipient spread.

To quantify the relative contribution of donor re-seeding and plasmid conjugation, we developed a mathematical model (Extended Data Fig. 6g). It assessed the interdependence of the donor-re-seeding rate (η, the sum of donor re-seeding plus the donor-to-recipient conjugation) and γ, the rate of transconjugant-to-recipient conjugation (see supplementary material). Fitting our mathematical model to the plasmid tag distributions confirmed that η is rate-limiting and identified the most likely parameters, i.e. $\eta = 3.16\times10^{-10}$ per day and $\gamma = 3.16\times10^{-8}$ per CFU/g feces per day (red in Fig. 3c; marginal posterior densities listed in Supplementary Table 4). This corresponds to ≈1.6 donor re-seeding (plus initial plasmid transfer) events per day into the gut lumen. In contrast, transconjugant-to-recipient plasmid conjugation rates were ≥32 per day (initial conjugations) and increase exponentially thereafter (see supplementary material).

We then employed our mathematical model to predict the effect of reducing the rate of donor re-seeding (η). The transconjugant-to-recipient conjugation parameter was fixed to $\gamma = 3.16\times10^{-8}$ per CFU/g feces per day (Fig. 3c), and we evaluated the probability of conjugation events to occur within the course of our 15-day experiment (Fig. 3d). Reducing

η by more than 100-fold diminished conjugation (Fig. 3d). To test this prediction, we employed oral vaccination with killed *S.*Tm cells[28], a procedure known to reduce *S.*Tm gut tissue invasion. In line with previous work [22], vaccinated mice contained 10-500 fold smaller persister reservoirs than naïve mice (Fig. 3e). Indeed, this prevented plasmid transfer in the vast majority of mice (Fig. 3f; Extended Data Fig. 7a-c). Moreover, the transconjugants detected in vaccinated mice appeared later than the transconjugants in non-vaccinated controls (Fig. 3f). Control experiments with reduced fractions of invasive donors verified this observation Extended Data Fig. 7d-g). Thus, the size of the tissue-associated persister reservoir is a main driver of the ensuing rise of transconjugants. These data confirm the predictions of our mathematical model (Fig. 3d) and suggest that vaccination might provide a means to prevent mucosa-associated conjugative plasmid reservoirs.

Next, we addressed if other microbiota strains could also acquire such plasmids. First, we analyzed P2^{cat} transfer to the commensal *E. coli* strain 8178 [20,22]. For this purpose, we created an ampicillin resistant, P2-plasmid free derivative of *E. coli* 8178 [20] and employed it as a recipient in the oral model (as in Fig. 1b). This yielded efficient plasmid transfer (Fig. 4a-b; Extended Data Fig. 8a). We tested if tissue-associated *S.*Tm persisters could also serve as the recipient. In the oral model (Fig. 1b), mice were first infected with a P2-cured variant of *S.*Tm SL1344 (Kan^R). Then, we treated with ciprofloxacin and ampicillin and introduced the donor (*E. coli* 8178 P2^{cat}; Amp^R; Cm^R). *S.*Tm re-seeded the gut lumen and transconjugants were formed (>38% median; Extended Data Fig. 8b-d). Thus, tissue-associated *S.*Tm persisters can serve as both donors or recipients of plasmid transfer between different Enterobacteriaceae.

To assess if mucosa-associated *S.*Tm can also serve as a reservoir for clinically relevant plasmids carrying extended spectrum beta-lactamase (ESBL) genes, we used pESBL15 (Extended Data Fig. 1b). *S.*Tm SL1344 pESBL15 was used as a donor. We modified our oral model from Fig. 1b in two ways: by replacing ampicillin with kanamycin in the drinking water and by using an ampicillin-sensitive, but kanamycin-resistant, variant of our standard recipient strain (*S.*Tm 14028S *aphT* (Kan^R, Amp^S)). We observed tissue-associated persisters, re-seeding of the gut-lumen and efficient plasmid transfer (Fig. 4c-d; Extended Data Fig. 8e). Thus, our findings apply to clinically important resistance plasmids. The choice of the antibiotics used for the different phases of our oral model had little effect on these fast plasmid transfer kinetics (Extended Data Fig. 9a-d).

Finally, we validated transfer of antibiotic resistance plasmids to *E. coli* in the I.V. model. I.V. infection of *S.*Tm P2^{cat} led to persistent populations in the internal organs (Fig. 4e) which migrated into the gut lumen and transferred the plasmid into the luminal recipient population, forming >25% *E. coli* transconjugants in the absence of antibiotic selection (Fig. 4f; Extended Data Fig. 9e). Thus, tissue-associated, *S.*Tm persisters can serve as reservoir for resistance plasmids that can be efficiently transferred to different Enterobacteriaceae.

Our results uncover a mechanism by which antibiotic persistence promotes the spread of antibiotic resistance plasmids, specifically by promoting the co-occurrence of donors and recipient bacteria in the gut luminal niche. This reveals an important new role of persistence in clinical bacterial infection: not only can bacterial persistence lead to relapse of disease in

chronic infections, but it can also facilitate the spread of antibiotic resistance. In our case, the transfer rate is independent of selective pressures for functions encoded on the plasmid. Thus, in absence of antibiotic-driven selection, resistance genes on promiscuous plasmids can spread from a very small number of donor cells co-occurring with dense recipient cell populations.

Mathematical modelling showed that re-seeding is the rate limiting aspect of this process, and suggested that reducing the tissue-associated population of *S.*Tm (e.g., through vaccination) could reduce plasmid re-seeding to negligible levels. As re-seeding events are rare compared to the number of tissue-associated persisters, such persister-promoted plasmid spread may last for weeks or months after an acute infection. So far, we do not know if this translates to livestock or human infections, where tissue-associated persister reservoirs might be smaller.

Associations between persistence and chronic infections happen in various clinical contexts [29] and biofilms [30]. Therefore, reservoirs for conjugative plasmids could exist in a multitude of persister populations. In our two mouse models, *S.*Tm persisters associated with different organs appear capable of gut-luminal re-seeding. The intracellular environment in classical dendritic cells [7] or macrophages [6] can induce persistence. In contrast to infected epithelial cells[31,32], these phagocytes are long-lived, suggesting they hold most of the persistent donors in both, the oral and the I.V. model. The differences between location of persister cell reservoirs in the oral model (lamina propria and mLN) and the I.V. model (spleen, liver, and gall bladder) and the differential requirement for SPI-1 and -2 encoded virulence factors indicate that there are diverse mechanisms by which tissue-associated *S.*Tm persisters can establish a reservoir, survive, and ultimately re-seed the gut lumen to engage in plasmid transfer.

The link between persistence and plasmid-mediated evolution of antibiotic resistance may be particularly relevant in the farming industry where *S. enterica* has a high prevalence, and animals are often co-colonized by *Salmonella* and *E. coli* strains. There can be two different *Salmonella* strains within the same host, one within lymphoid tissues (e.g. mesenteric lymph nodes) and the other in the intestinal content [17]. This is also in line with the isolation of *Salmonella spp.* from intestinal biopsies in swine with persistent subclinical *Salmonella* infections, indicating that pathogen persister reservoirs are common in the gut mucosa of these animals [15,16]. Our results suggest that this may promote the spread of resistance plasmids in animal herds.

Strategies to reduce bacterial persistence are of general importance (reviewed in [33]). This is relevant not only for the clinical treatment of infected individuals [29], but also to minimize the impact of persistence on the global evolution of antibiotic resistance via both resistance mutations [11] and resistance plasmid spread (this work). Inactivated vaccines such as the peracetic acid killed *Salmonella* cells used herein, should be easily and safely applicable [28]. Our data show that vaccination efficiently prevents not only tissue invasion and disease, but also minimizes tolerant reservoirs and subsequent resistance (e.g. ESBL-encoding) plasmid spread (Fig. 3).

Materials and methods

Strains and plasmids used in this study

Supplementary table 1 contains all strains and plasmids used in this study. For cultivation of bacteria, lysogeny broth (LB) media containing the appropriate antibiotics (50 μg/ml streptomycin (AppliChem); 6 μg/ml chloramphenicol (AppliChem); 50 μg/ml kanamycin (AppliChem); 100 μg/ml ampicillin (AppliChem)) were used. In order to create P2^{cat} TAG strains (using neutral genetic barcodes from [34]) or gene deletion mutants (e.g. *oriT::aphT* on P2), the λ *red* system was used as described in [35]. If desired, antibiotic resistance cassettes were removed using the temperature-inducible FLP recombinase encoded on pCP20 [35]. Mutations or sequence tags coupled to antibiotic resistance cassettes were transferred into the desired genetic background using transduction with P22 HT105/1 *int-201* [36]. Primers used for strain construction or verification of genetic background are listed in Supplementary table 2.

In vitro plasmid transfer kinetics

Overnight cultures with appropriate antibiotics of donor (SL1344 P2^{cat}) and recipient (14028S *aphT*) strains carrying pM975 to confer ampicillin resistance were subcultured 1:20 in LB without antibiotics and grown for 4 hours. Approximately 10^2 CFU of each were added (sequentially as 25 μl volumes) to 450 μl LB with 100 μg/ml ampicillin. Samples were incubated at 37°C mixing at 1000 rpm for 24 hours. Aliquots (10 μl) were taken every hour, diluted, and plated on selective MacConkey agar for enumeration.

In vitro antibiotic resistance profiling

Flat-bottom transparent 96-well plates were filled with 100 μl of LB containing 2-fold dilutions of the specified antibiotic (streptomycin (AppliChem), chloramphenicol (AppliChem), kanamycin (AppliChem), ampicillin (AppliChem), ciprofloxacin (ciprofloxacin hydrochloride monohydrate; Sigma-Aldrich), gentamycin (AppliChem), or ceftriaxone (ceftriaxone disodium salt hemi(heptahydrate); Sigma-Aldrich). Each plate contained 11 2-fold dilution steps of each antibiotic, plus a no antibiotic control, and a no-bacteria sterility control. Overnight cultures of each bacterial strain tested were grown in the presence of appropriate antibiotics, subcultured (1:20 dilution) for 4 hours at 37°C in LB without antibiotics, and diluted in PBS. Cells were seeded in each well at a final density of 10^5 CFU/ml. 96-well plates were incubated at 37°C at 120 rpm for 16 hours and the $OD600_{nm}$ was measured. The no-bacteria sterility control was used for background subtraction.

Infection experiments

Oral infection model—For *in vivo* plasmid transfer experiments, 8-12 week old 129Sv/Ev mice were used. These mice are *Nramp1*$^{+/+}$ and therefore allow for long-term *S.*Tm infections [37]. They carry a complex specified pathogen free microbiota without *E. coli*. The experiment has three phases, i.e., 1) donor colonization, 2) clearance with antibiotics, and 3) recipient colonization and conjugative transfer. Phase 1: Animals were pretreated with 25 mg streptomycin orally to allow for robust colonization of *S.*Tm [38].

Donor (i.e., plasmid-bearing) *S.*Tm were cultivated overnight at 37°C in LB containing the appropriate antibiotics, subcultured (1:20 dilution) for 4 hours at 37°C in LB without antibiotics, washed with sterile PBS, and $5x10^7$ CFU were introduced into mice via oral gavage [38]. Phase 2: Two days post infection, 3 mg of ciprofloxacin (ciprofloxacin hydrochloride monohydrate; Sigma-Aldrich) dissolved in 100 µl sterile dH_2O was administered by oral gavage for three consecutive days. Mice were transferred to fresh cages after each ciprofloxacin treatment to minimize gut recolonization from the environment. Ampicillin (2 g/l) or kanamycin (1 g/l) was added to the drinking water starting at day 3 post infection and maintained until either day 8 or day 15. This prevented premature donor re-seeding after the cessation of ciprofloxacin treatment. Phase 3: Mice were kept individually after ciprofloxacin treatment to prevent cross-contamination due to coprophagy. Recipient bacteria (i.e., plasmid-free *S.*Tm or *E. coli*; $5x10^7$ CFU) were orally introduced into mice on day 8 post infection (culture and subculture conditions as above) and populations are monitored for 7 days until sacrifice (day 15).

I.V. infection model—The in vivo plasmid transfer experiment has three phases, i.e. 1) donor colonization, 2) clearance with antibiotics, and 3) recipient colonization and conjugative transfer. Phase 1: The donor strain is injected intravenously into the tail vein of 8-12 week old 129Sv/Ev mice (10^3 CFU). Phase 2: 2 days after I.V. infection of donors, 1.5 mg of ceftriaxone (ceftriaxone disodium salt hemi(heptahydrate); dissolved in 100 µl PBS; Sigma-Aldrich) was intraperitoneally injected for three consecutive days. After the third treatment, mice were transferred to fresh cages and kept individually to prevent cross-contamination due to coprophagy. Phase 3: the recipient is introduced on day 7 post donor infection (10^8 CFU by gavage) and fecal populations are monitored for 18 days until sacrifice (day 25).

In both infection models, feces were collected daily, homogenized in PBS with a steel ball at 25 Hz for 1 minute, diluted, and selective plating on MacConkey agar (supplemented with the appropriate antibiotics) was used to enumerate populations of donors, recipients, or transconjugants. The proportion of transconjugants was calculated by dividing the transconjugant population (Cm^R, Kan^R) by the sum of transconjugants and plasmid-free recipients (Kan^R). Lipocalin-2 ELISA (R&D Systems kit; protocol according to manufacturer) was performed on feces to determine the inflammatory state of the gut. Upon sacrifice (at day 5, 8, 15, or 25; specified in each figure legend), the mesenteric lymph nodes, spleen, liver, and gall bladder were collected, homogenized in PBT at 25 Hz for 2 minutes, and bacteria were enumerated by selective plating. The cecum was removed, opened longitudinally, washed 3 times in PBS, and then placed in 400 µg/ml gentamycin (AppliChem) for 30 minutes at room temperature. 9 consecutive washing steps in PBS (45 seconds each) ensured removal of gentamycin; cecal tissue was subsequently homogenized and mucosa-associated bacteria were enumerated as for the other organs (gentamycin protection protocol modified from [24]). In Extended Data Fig. 5a, additional organs were collected as indicated in the figure legend. All organs were processed as indicated above. For the jejunum, ileum, and colon, 1 cm of intestine was harvested, washed briefly in PBS and the tissue (including the majority of the content) was analyzed. For analysis of bacteria in

the blood, 100 µl of blood was aspirated from the heart immediately after sacrifice and mixed in PBS containing 2% BSA and 1 mM EDTA to prevent coagulation.

For competition experiments, 8-12 week old 129 SvEv mice were pretreated with 20 mg ampicillin orally, and ampicillin (2 g/l) was maintained in the drinking water throughout the experiment. The two competitor strains were cultured separately in LB containing the appropriate antibiotics, subcultured, and washed with PBS, as above. Strains were mixed at a 1:1 ratio immediately before gavaging $5x10^7$ CFU of the mixture into the ampicillin pretreated mice. Feces were monitored daily, homogenized, and enumerated by selective plating. Competitive index was calculated by the ratio of population sizes of competitors at the indicated time. Mice were sacrificed after 7 days.

All animal infection experiments were approved by the responsible authority (Tierversuchskommission, Kantonales Veterinäramt Zürich, license 193/2016). Sample size was not predetermined. Mouse age and gender were matched between treatment groups and animals were randomly distributed among groups. In four cases, data from mice were excluded since the animals needed to be sacrificed prematurely due to disease or symptom severity.

Confocal microscopy

To visualize persisters in the cecum lamina propria, cecum tissues were fixed in PBS/4% paraformaldehyde, saturated in PBS/20% sucrose and embedded in optimum cutting temperature medium (OCT, Tissue-Tek) before being flash-frozen in liquid nitrogen. 10 µm cryosections were air-dried, rehydrated with PBS, permeabilized with PBS/0.5%Triton X-100 and blocked with PBS/10% Normal Goat Serum. α-*S.*Tm LPS O5 (Difco), α-*S.*Tm LPS O12 (STA5; [22]), α-ICAM-1/CD54 (BD Biosciences), appropriate secondary antibodies, DAPI (Sigma Aldrich) and AlexaFluor488-conjugated phalloidin (Santa Cruz) were used for the staining. A Zeiss Axiovert 200m microscope with 10x–100x objectives, a spinning disc confocal laser unit (Visitron), and two Evolve 512 EMCCD cameras (Photometrics) were used for acquiring images. Images were processed using Visiview (Visitron). LPS positive (O5-positive and/or O12-positive) *S.*Tm were manually enumerated blindly in 8-12 nonconsecutive sections per mouse. Phalloidin and ICAM-1 staining were used to differentiate the lamina propria and epithelium. All data represent averages per section.

Mucus fixation and staining

Cecal tissue samples were fixed with freshly prepared Methacarn solution (60% methanol, 30% chloroform, 10 % glacial acetic acid) for 24 hours at room temperature [39]. The samples were transferred to methanol for 2 hours and processed over night with a LogosJ tissue processor (Milestone) using the following program:

30 min	37°C EtOH
30 min	37°C EtOH
60 min	37°C EtOH

60 min	40°C Isopropanol	15 min for heating up
60 min	45°C Isopropanol	20 min for heating up
180 min	68°C Isopropanol	20 min for heating up
240 min	82°C Paraffin	75 min for heating up

The paraffinized tissue was then embedded as paraffin blocks for further storage. 10 μm sections were deparaffinized in Xylene substitute solution (Sigma-Aldrich) for 20 minutes. The sections were rehydrated in sequential baths of 100%, 95%, 70%, 50% and 30% ethanol for 5 minutes each and subsequently incubated for 10 min in PBS. For mucus visualization, the sections were stained with DAPI, phalloidin-FITC, Wheat germ agglutinin (WGA) AF647 conjugate (Invotrogen, Cat#W32466), Rabbit polyclonal anti-Salmonella O5 (Becton Dickinson, Cat#226601) and Goat polyclonal anti-Rabbit Fab Cy3 conjugate (Jackson ImmunoResearch Labs, Cat# 111-167-003; RRID: AB_2313593) antibodies.

Analysis of plasmid transfer dynamics

Mice were orally or I.V. infected with a mixture of 5 isogenic SL1344 P2$^{cat\ TAG}$ strains (tags at a 1:1:1:1:1 ratio; inoculum made of approximately 10^7 CFU each tagged strains for oral infection and 2×10^2 CFU each tagged strain for I.V. infection) using the same oral model or I.V. model protocol described above (Fig. 1b, 2b). On day 8 (oral model), mice were gavaged with a mixture of 5 recipient strains (14028S *TAG*; Kan^R; Amp^R; tags at 1:1:1:1:1 ratio; inoculum approximately 10^7 CFU each tag). Barcode analysis of the recipient chromosome tags could not be performed for technical issues with kanamycin enrichments and subsequent qPCR. In the I.V. model, the recipient used was not tagged, but was introduced on day 7 (10^8 CFU by oral gavage). The plasmid and recipient tags can be easily distinguished since the primer pairs used for qPCR are unique (i.e., WITSX-R paired with Cat_internal for P2 tags; WITSX-R paired with Kan_internal for recipient tags; in the IV model where recipient tags were not used, WITSX was paired with ydgA for qPCR as there was no need for antibiotic resistance-specific qPCR primers). For the oral model, the inoculums, feces at day 1, 9, and 15, as well as cecal tissue after gentamycin treatment was enriched overnight in 5 ml LB containing the appropriate antibiotics (donors = Sm+Cm; recipients = Kan; transconjugants = Cm+Kan) in parallel to selective plating to enumerate bacterial population sizes. For the I.V. model, the donor inoculum, as well as feces, gall bladder, liver, spleen, mLN, and cecal tissue at sacrifice (day 25) were enriched in LB with the appropriate antibiotics.

Enrichments were concentrated and genomic DNA was extracted using a QIAamp DNA Mini Kit (Qiagen). qPCR analysis was performed using temperature conditions described previously [34]. qPCR primers are listed in Supplementary table 2. For each sample, 5 primer pairs were used to amplify P2 tags (in the oral model WITSX-R with Cat_internal, where X is 2, 11, 13, 19, or 21; in the IV model WITSX with ydgA where X is 2, 11, 13, 19, or 21). Primers were modified from the original WITS primers described in [34]; tag loci remain the same as in [34]. Relative proportion was determined by dividing the DNA copy number (calculated from the C_T value; a dilution standard of purified chromosomal DNA allowed for a correlation between DNA copy number and C_T value) of each tag detected by the sum of

Europe PMC Funders Author Manuscripts

Europe PMC Funders Author Manuscripts

all tags in the sample. The detection limit was determined by the C_T value of the most diluted DNA standard (linearity of the standard curve decreases dramatically below this value) for each qPCR run. The least precise detection limit constitutes the conservative detection limit used for fitting our mathematical model (2.9×10^{-3}). Plasmid tags were ranked according to frequency (Extended Data Fig. 6c) as the strains are isogenic (except for the tag), and each mouse can be treated as an independent realization of the stochastic population dynamics. The data of plasmid tag frequencies and the bacterial population counts were used to parametrize a mechanistic model of the plasmid re-seeding dynamics, and infer the most likely rates of donor re-seeding (including initial plasmid transfer) and transconjugant-to-recipient transfer (Extended Data Fig. 6g; a detailed description is given in the supplementary materials).

Oral vaccination

Peracetic acid inactivated oral vaccines were prepared as described previously [28]. *S.*Tm was grown overnight and concentrated to 10^{10} CFU/ml in PBS. Peracetic acid (Sigma-Aldrich) was added to a final concentration of 0.4% v/v, mixed vigorously, and incubated at room temperature for 2 hours. Traces of acid were removed after inactivation by washing bacteria with sterile PBS three times. Inactivated bacteria were resuspended at 10^{11} particles per ml in sterile PBS. Complete inactivation was ensured by inoculating a 100 µl dose of vaccine into 50 ml LB and checking for sterility. Vaccines were stored at 4°C for up to 2 months. Mice received a 100 µl dose of vaccine by oral gavage once per week for 5 weeks. Naïve control mice were mock-vaccinated with PBS.

Statistical analysis

Statistical tests on experimental data were performed using GraphPad Prism 7 for Windows. Fitting of the mathematical model to experimental values was performed using an Approximate Bayesian Computation (ABC) approach [40]. Transfer rates were varied on a grid from 10^{-12} – 10^{-1}; the summary statistics consist of the skew of the plasmid tag abundance distribution, the fraction of tags above the detection limit on day 15, the total size of the transconjugant population on day 15, as well as the time at which the transconjugant population size first exceeds 10^6 CFU/g feces. A simulation is called “successful” if all summary statistics are within three standard deviations of the experimentally observed mean of these statistics. All R-code needed to simulate the stochastic model, estimate the most likely parameters from the experimental data, and plot the results, is included in the attached zip-folder.

Extended Data

Europe PMC Funders Author Manuscripts

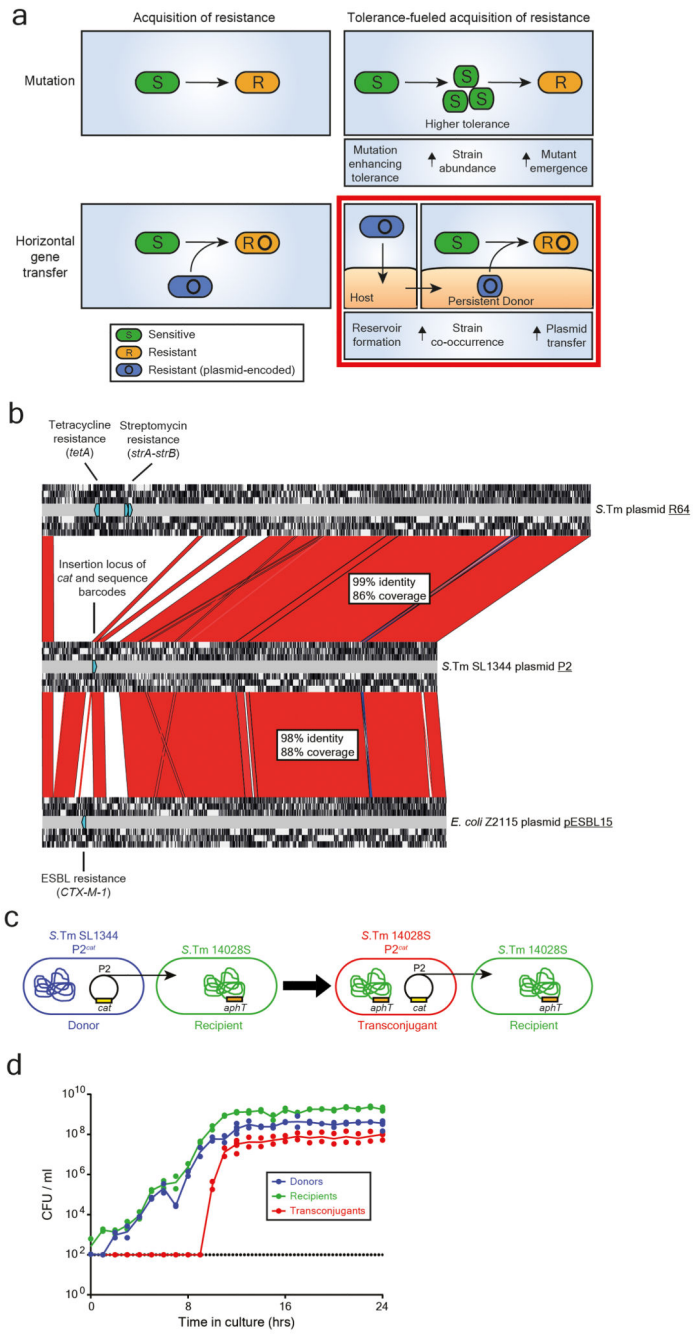

Extended data Fig. 1. Emergence and spread of antibiotic resistance in bacteria using P2 as a model for conjugation.

a) Antibiotic resistance in bacteria can emerge through mutation or be acquired via horizontal gene transfer. Plasmid transfer is an important driver of the spread of antibiotic resistance. Tolerance increase the abundance of bacteria that survives antibiotic exposure, allowing for a higher probability of emergence of mutations leading to resistance [11]. We hypothesize that antibiotic resistance can also spread through the formation of reservoirs of persistent bacteria containing plasmids (here, we hypothesize that the host gut mucosa can serve as a reservoir for persisters). The formation of long-term reservoirs, followed by re-

seeding of bacteria from this reservoir into a niche occupied by other bacteria (e.g. the gut lumen occupied by the microbiota following antibiotic therapy) increases the chance that two different strains interact with each other, leading to plasmid transfer (i.e., increased strain co-occurrence). The graphical representation of the bottom right panel is an example for persistent donors boosting co-occurrence. Please note that persistent, tissue-associated recipients may also increase co-occurrence. **b)** P2 shares homology with resistance plasmids. An alignment is shown between *S.*Tm SL1344 P2 (GenBank sequence ID: HE654725.1), *S.*Tm plasmid R64 (GenBank sequence ID: AP005147.1), and pESBL15 of *E. coli* Z2115 (strain isolated from a rectal swab of a patient at the University Hospital Basel) using Artemis Comparison Tool (https://www.sanger.ac.uk/science/tools/artemis-comparison-tool-act). Red fill indicates high sequence identity (>85% sequence identity), blue fill indicates inversions, and no fill indicates no sequence identity. For each plasmid, open reading frames (in each of the 6 translational frames) are shown by white regions (detected by Artemis Comparison Tool). Antibiotic resistances (e.g. streptomycin and tetracycline resistances on R64 and *CTX-M-1* on pESBL15) are labelled, shown by light blue directed rectangles (found by a Basic Local Alignment Search Tool (NCBI) search against the ResFinder antibiotic resistance gene database [41]). In P2, the locus for insertion of the chloramphenicol resistance cassette and neutral sequence tags. For each alignment, the percentage of the sequence that aligns to P2 is shown, as well as the average sequence similarity for these regions. **c)** Model strains for addressing evolution by conjugation in *S.*Tm. SL1344 contains P2^{cat} (chloramphenicol resistance cassette (*cat*) allows enumeration of plasmid bearing strains by selective plating) that can be conjugated to 14028S (kanamycin resistance cassette (*aphT*) used for selective plating) to form a transconjugant (Cm^{R}, Kan^{R}). Transconjugants can then transfer P2^{cat} to more recipients. **d)** P2^{cat} transfer kinetics *in vitro*. P2^{cat} transfer is dependent on the density of donors and recipients. Donor and recipient strains were inoculated into LB (n=2) at a 1:1 ratio and selective plating was performed every hour. CFUs per ml are reported for each population (donors in blue; recipients in green; transconjugants in red). Solid lines connect medians. Dotted line indicates detection limit by selective plating.

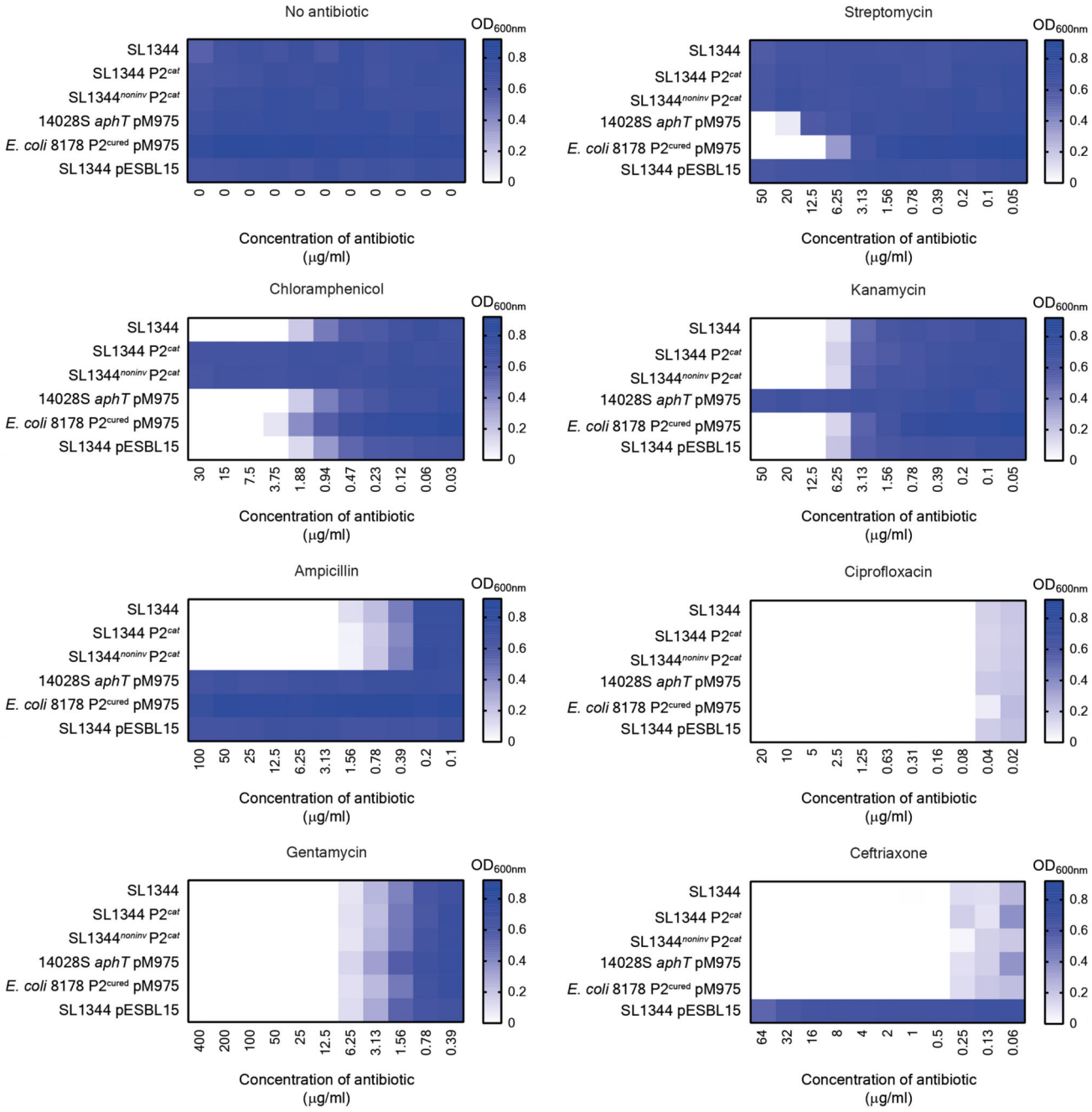

Extended data Fig. 2. Antibiotic resistance profile of key strains.

Antibiotic susceptibility testing was performed in LB in 96-well plates. 6 strains (indicated in the figure axis) were tested against 7 antibiotics, grown at 37°C at 120 rpm for 16 hours when the OD_{600nm} was measured. For each antibiotic, the highest concentration used was based on the working concentration in this study. For example, the concentration of antibiotic used for selective plating in the case of streptomycin, kanamycin, ampicillin, and chloramphenicol (the highest concentration of chloramphenicol was 5-fold higher than the concentration used for selective plating, since this was already close to the minimum

inhibitory concentration), or the concentration of antibiotic used for the gentamycin protection assay. Importantly, a very low minimum inhibitory concentration was observed for antibiotics used *in vivo* to enrich for persisters (i.e., ciprofloxacin and ceftriaxone). The mean of three experiments is presented on a blue-white colour gradient, where blue indicates a large amount of bacterial growth. This is calculated by subtracting the OD_{600nm} measured for each sample well subtracted by the background generated by the media.

Europe PMC Funders Author Manuscripts

Europe PMC Funders Author Manuscripts

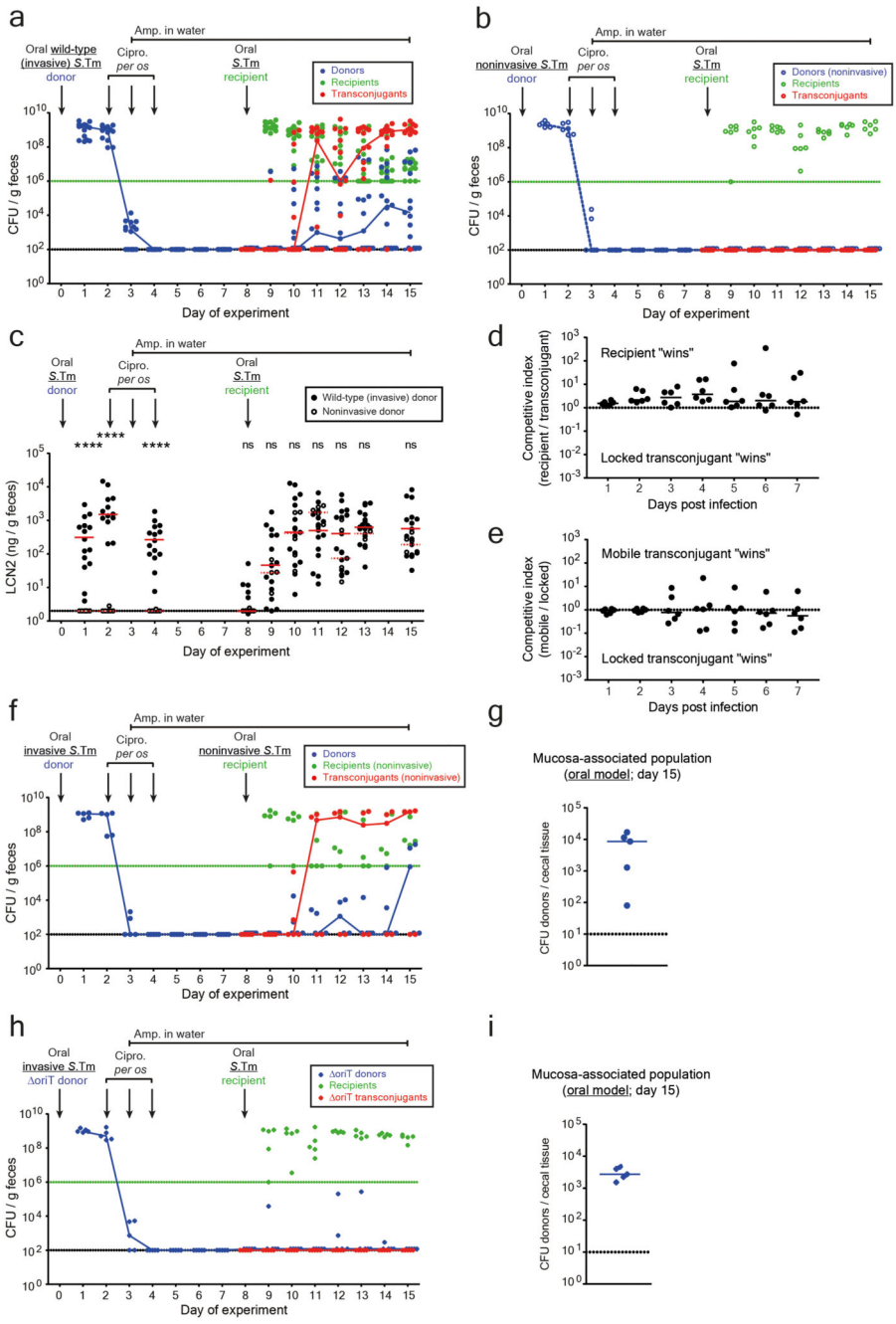

Extended data Fig. 3. Controls for conjugation after antibiotic treatment in the oral infection model.

a-c) Fecal bacterial population sizes and inflammatory status of mice in Figure 1c-d (comparison of invasive vs. noninvasive donors in the oral model). Fecal loads of donors (blue; Sm^R, Cm^R), recipients (green; Kan^R), and transconjugants (red; Cm^R, Kan^R) were determined by selective plating on MacConkey agar. Black dotted line indicates detection limits for donors and transconjugants. Green dotted line indicates detection limit for recipients (the detection limit is higher for recipients once transconjugants reach a density of

>10^8 CFU/g feces. Before this happens, recipients can be found below the detection limit and then the black dotted line should be considered as the detection limit). Blue lines connect medians of donor populations; red lines connect medians of transconjugant populations. **a**) Mice infected with invasive *S.*Tm donors (solid circles; n=15 singly housed mice from five independent experiments). **b)** Mice infected with noninvasive *S.*Tm donors (open circles; n=6 singly housed mice from two independent experiments). **c)** Inflammatory status was determined by lipocalin-2 ELISA. Statistics are performed using a two-tailed Mann-Whitney U test p>0.05 (ns), p<0.0001 (****) comparing mice infected with an invasive donor (solid black circles; n=15 singly housed mice from five independent experiments) to mice infected with a noninvasive donor (open black circles; n=6 singly housed mice from two independent experiments) at each time point. Medians are shown (solid red line for invasive donors; dotted red line for noninvasive donors). Dotted line indicates detection limit. **d-e)** Carrying P2^{cat} does not lead to a measurable fitness cost or benefit. **d)** A "locked" transconjugant (14028S P2$^{aphT\ \Delta oriT}$; conjugation is blocked by removing the origin of transfer; Kan^R, Amp^R) was competed against a recipient (14028S *cat*; Cm^R, Amp^R). **e)** To ensure removing the origin of transfer did not affect fitness, the locked transconjugant was competed against a transconjugant with a normal P2^{cat} plasmid (i.e., mobile transconjugant) (14028S P2^{cat}; Cm^R, Amp^R). In **panel d-e**, both strains were introduced at a 1:1 ratio (total inoculum size ~5×10^7 CFU *per os*) and feces were monitored daily by selective plating (n=6 singly housed mice from two independent experiments for both experiments). Competitive index is calculated by dividing the population size of one competitor by the other. Lines indicate medians. The dotted line indicates no competitive advantage for either strain. This is in line with published data [20]. These data indicate that it is the plasmid-encoded conjugation efficiency (not its effects on host bacterial fitness) that drives the prodigal rise of transconjugants (Fig. 1c). **f-g)** Plasmid transfer in the oral model does not require an invasive recipient. Invasive donors (SL1344 P2^{cat}; Sm^R, Cm^R) were orally infected into pretreated mice. After ciprofloxacin treatment, a noninvasive mutant of *S.*Tm 14028S was used as a recipient (14028S^{noninv} *aphT* (Kan^R, Amp^R); n=5). **f)** Selective plating determined fecal loads of donors (blue; Sm^R, Cm^R), recipients (green; Kan^R), and transconjugants (red; Cm^R, Kan^R). Black dotted line indicates detection limit for donors and transconjugants. Green dotted line indicates detection limit for recipients (the detection limit is higher for recipients once transconjugants reach a density of >10^8 CFU/g feces. Before this happens, recipients can be found below the detection limit and then the black dotted line should be considered as the detection limit). Blue lines connect medians of donor populations; red lines connect medians of transconjugant populations. **g)** Donor populations enumerated after a gentamycin protection assay on cecal tissue of mice shown in **panel f**. Median indicated by solid line. Dotted line indicates detection limit. **h-i)** conjugation is required for plasmid transfer after antibiotic treatment. Mice were infected with invasive *S.*Tm lacking the origin of transfer in P2^{cat} (SL1344 P2$^{cat\ \Delta oriT}$; Sm^R, Cm^R) as a donor, and 14028S *aphT* (Kan^R, Amp^R) as a recipient after antibiotic treatment (n=5). **h)** Selective plating determined fecal loads of donors (blue; Sm^R, Cm^R), recipients (green; Kan^R), and transconjugants (red; Cm^R, Kan^R). Black dotted line indicates detection limit for donors and transconjugants. Green dotted line indicates detection limit for recipients (the detection limit is higher for recipients once transconjugants reach a density of >10^8 CFU/g feces. Before this happens, recipients can be found below the detection limit and then the black dotted line

should be considered as the detection limit). Blue lines connect medians of donor populations; red lines connect medians of transconjugant populations. **i)** Donor populations enumerated after a gentamycin protection assay on cecal tissue of mice shown in **panel h**. Median indicated by solid line. Dotted line indicates detection limit.

Europe PMC Funders Author Manuscripts

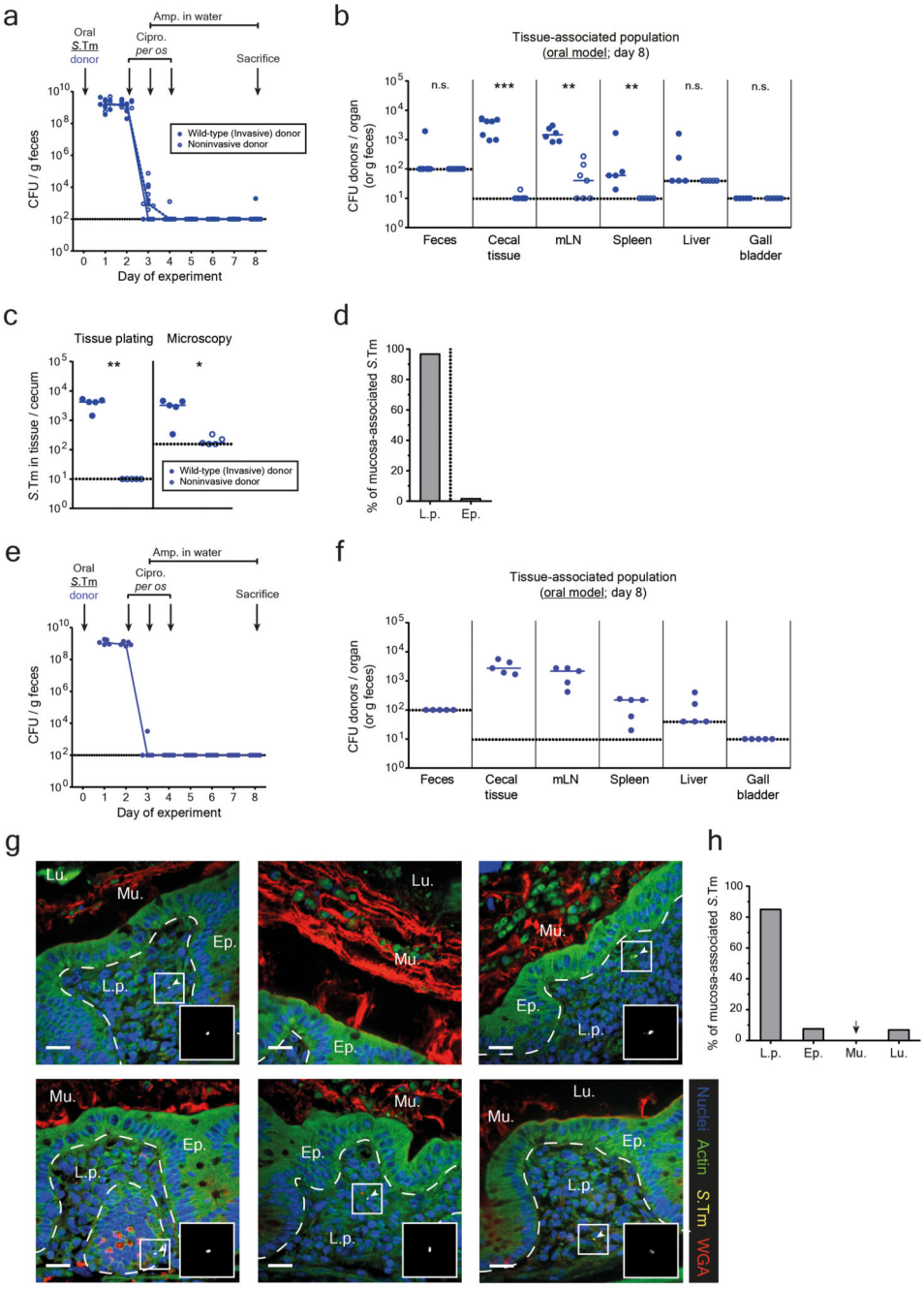

Extended data Fig. 4. Quantification and localization of *S*.Tm in the host mucosa after antibiotic treatments in the oral model.

a-d) Mice were orally infected with either an invasive (SL1344 P2^{cat}; blue solid circles; n=7) or noninvasive (SL1344^{noninv} P2^{cat}; T3SS-1 negative; blue open circles; n=7) donor and treated with antibiotics. Mice were sacrificed at day 8 after infection (when recipients are normally added) and organs were analyzed. Dotted lines indicate detection limits. **a)** Fecal populations were monitored daily by selective plating on MacConkey agar. Blue lines connect medians. **b)** Organ loads were determined by selective plating. mLN: mesenteric

Europe PMC Funders Author Manuscripts

lymph nodes. **c)** Population size of donors in the cecal mucosa determined by selective plating after a gentamycin protection assay or microscopy of tissue sections (same mice for each quantification method). Each data point is the average of 12 sections (10 μm thick). **Panel b-c)** Statistics are performed using a two-tailed Mann-Whitney U test $p>0.05$ (ns), $p<0.05$ (*), $p<0.01$ (**), $p<0.001$ (***), $p<0.0001$ (****) comparing mice infected with invasive or noninvasive donors for each organ. **d**) Localization of *S.*Tm detected in the cecal tissue by microscopy, reported as a percentage of bacteria detected in **panel c** in either the lamina propria (L.p.) or epithelium (Ep.). Bar indicates the median from 5 mice. **e-h)** Analysis of persister reservoirs in Carnoy-fixed cecal tissue sections. Mice were orally infected with an invasive (SL1344 P2^{cat}; n=5) donor and treated with antibiotics. Mice were sacrificed at day 8 after infection (when recipients are normally added) and organs were analyzed. Dotted lines indicate detection limits. **e)** Fecal populations were monitored daily by selective plating on MacConkey agar. Blue lines connect medians. **f)** Organ loads were determined by selective plating. mLN: mesenteric lymph nodes. Line indicates median. **g)** A Carnoy fixation was performed on ceca of mice to preserve the mucus structure. 10 μm sections were stained to visualize *S.*Tm (yellow; α-LPS O5), actin (green; phalloidin-FITC), the mucus (red; wheat germ agglutinin (WGA) AF647 conjugate), and nuclei (blue; DAPI). Ep., epithelium; Lu., Lumen; L.p., lamina propria. Mu., mucus. Scale bars represent 20μm. White arrows highlight *S.*Tm (magnified in inset). Representative images shown from two independent experiments. **h)** Localization of *S.*Tm detected in the cecal tissue by microscopy, reported as a percentage of bacteria detected each section (12 sections per mouse cecum) in the lamina propria (L.p.), epithelium (Ep.), mucus (Mu.), or lumen (Lu.). Bar indicates the median from 5 mice.

Europe PMC Funders Author Manuscripts

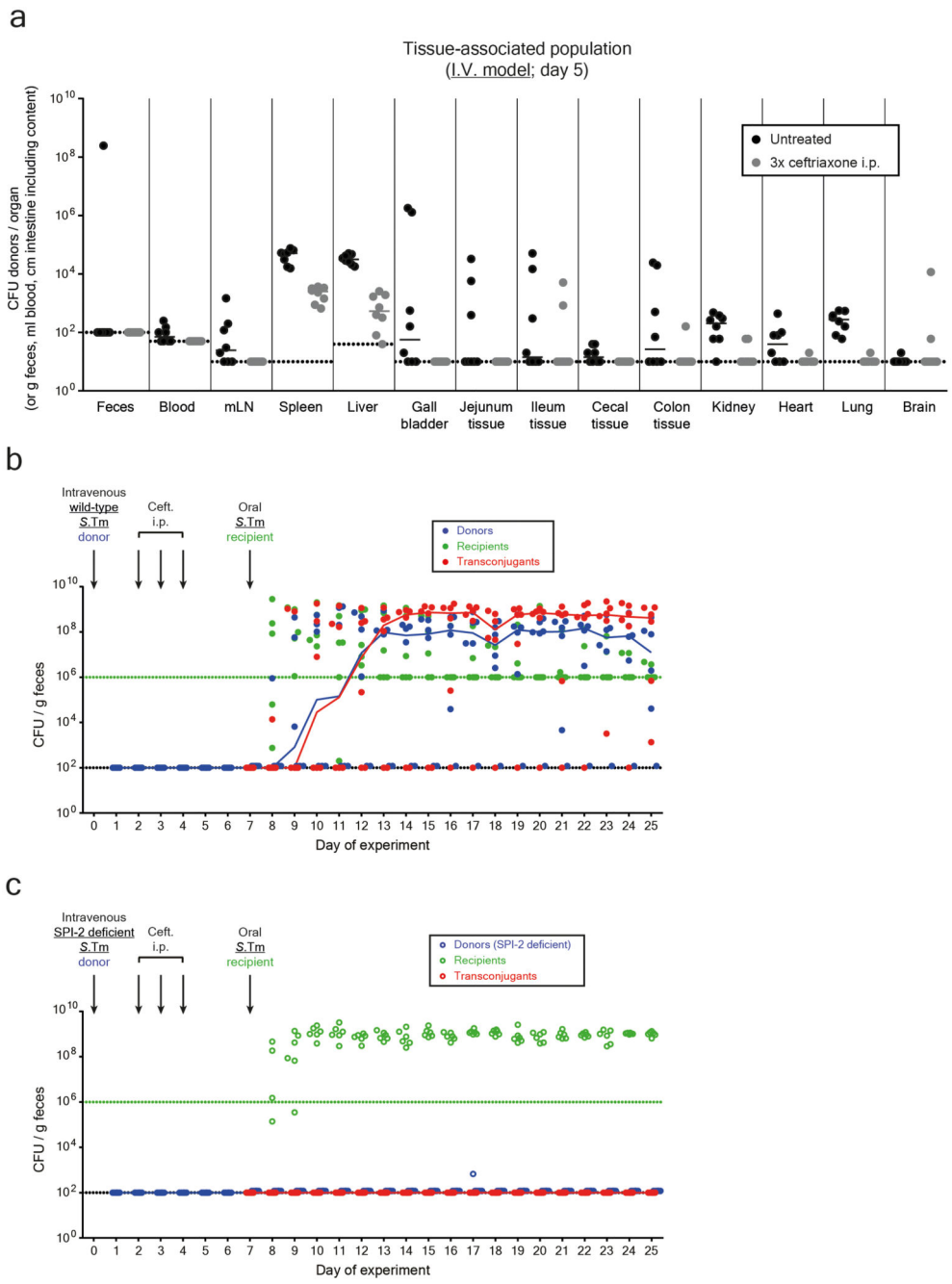

Extended data Fig. 5. Determination of tissue-associated persister reservoirs after I.V. infection, and subsequent plasmid transfer.

a) An equal mix of five SL1344 P2$^{cat\ TAG}$ strains (Sm^{R}, Cm^{R}) were I.V. infected into mice (10^{3} CFU). Treatments were as described in Fig. 2b (grey circles; 3 doses of ceftriaxone i.p.; n=8 singly housed from two independent experiments), or mice were left untreated (black circles; n=8 singly housed from two independent experiments). Mice were sacrificed on day 5 of the experiment (after the final dose of ceftriaxone was given). The tissue-associated populations in organs were enumerated by selective plating. Detection limit by selective

plating is shown as a dotted line. Lines indicate median. **b-c)** Fecal bacterial population sizes of mice in Figure 2D-E (comparison of wild-type vs. SPI-2 negative donors in the I.V. model). Fecal loads of donors (blue; Sm^R, Cm^R), recipients (green; Kan^R), and transconjugants (red; Cm^R, Kan^R) were determined by selective plating on MacConkey agar. Black dotted line indicates detection limits for donors and transconjugants. Green dotted line indicates detection limit for recipients (the detection limit is higher for recipients once transconjugants reach a density of $>10^8$ CFU/g feces. Before this happens, recipients can be found below the detection limit and then the black dotted line should be considered as the detection limit). Blue lines connect medians of donor populations; red lines connect medians of transconjugant populations. **b**) Mice infected with wild-type *S.*Tm donors (solid circles). **c)** Mice infected with SPI-2 deficient *S.*Tm donors (open circles).

Europe PMC Funders Author Manuscripts

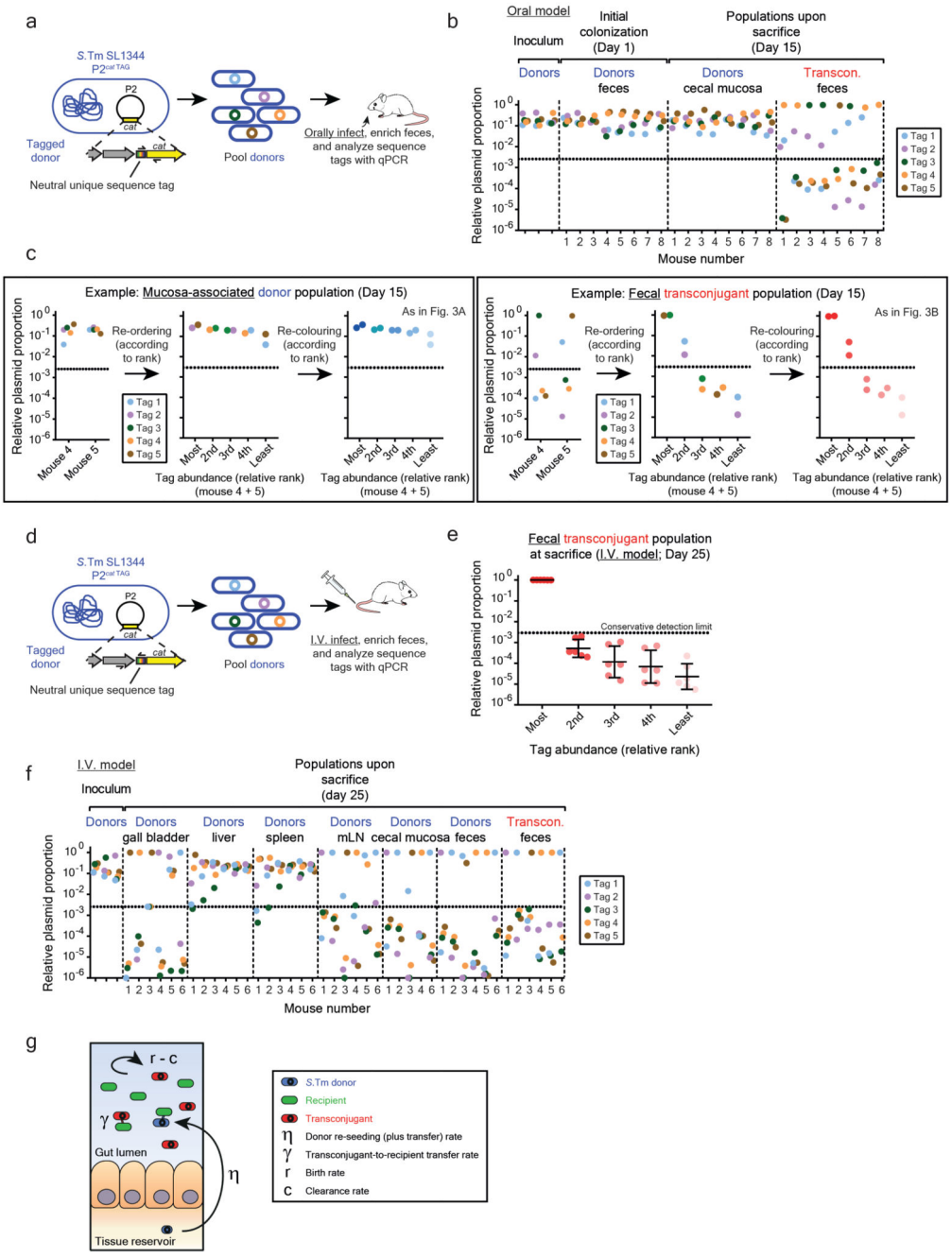

Extended data Fig. 6. Experimental strategy for assessing population dynamics and tag frequencies for figure 3a-d.

a-c) Tags introduced in the oral model. **a)** Tags coupled to a chloramphenicol resistance cassette were introduced in P2. qPCR primers are specific to the chloramphenicol resistance cassette and the specific tag (shown as one-sided arrows). Five tagged donors were pooled and orally infected as a 1:1:1:1:1 mix into mice. **b)** Relative plasmid tag proportion detected by qPCR in the initial donor population, the donor population persisting in the cecal mucosa, and the transconjugant population is shown for 8 mice (3 independent inocula). Dotted line

Europe PMC Funders Author Manuscripts

indicates the detection limit. Each tag is given a unique colour. **c)** Scheme illustrating how tags were sorted and recoloured to yield the plots in Fig. 3a-b. Two mice are shown as examples. For both mucosa-associated donor populations (top panel) and fecal transconjugant populations (bottom panel), tags were sorted according to relative frequency. These tags were re-coloured (darker colour indicates higher frequency) in order to visualize the trends shown in Fig. 3a-b. These re-ordered tags were used as the experimental data for fitting the mathematical model. **d-f)** Experimental strategy to assess plasmid transfer dynamics in the I.V. model. **d)** Tags coupled to a chloramphenicol resistance cassette were introduced in P2. qPCR primers are specific to *ydgA*, a pseudogene flanking the specific tags, and the specific tag (shown as one-sided arrows). Five tagged donors were pooled and I.V. infected as a 1:1:1:1:1 mix into mice. **e)** Tags from the fecal transconjugant population at day 25 are sorted by abundance. Note that each abundance rank can consist of any tag (see ranking and re-colouring scheme in **panel c;** raw tag data in **panel f** of this figure**;** n=6 singly housed mice from two independent experiments). Dotted line indicates conservative detection limit by qPCR. This detection limit refers to the most conservative detection limit of any qPCR run (2.9×10^{-3}; i.e., tags can appear below this detection limit if the qPCR run yielded a lower detection limit). Line indicates mean; error bars indicate standard deviation. **f)** Relative plasmid tag proportion detected by qPCR in the inoculum, the donor population persisting in the internal organs, and the transconjugant population in the feces is shown for 6 mice (3 independent inocula; feces and organ population data in Fig. 2d). Dotted line indicates the detection limit. Each tag is given a unique colour. **g)** Graphical representation of key parameters in the mathematical model. Donors form a persistent reservoir in host tissues. These cells can interact with other bacteria colonizing the gut lumen (i.e., recipients) and transfer plasmids. Our mathematical model summarizes these plasmid transfer dynamics using a few key parameters. Donors re-seed the gut lumen and transfer plasmids at rate η, transconjugants transfer plasmids to recipients (without a plasmid) with rate γ, and the turn-over of each bacterial population is given by r-c, where r is the birth rate and c the clearance rate.

Europe PMC Funders Author Manuscripts

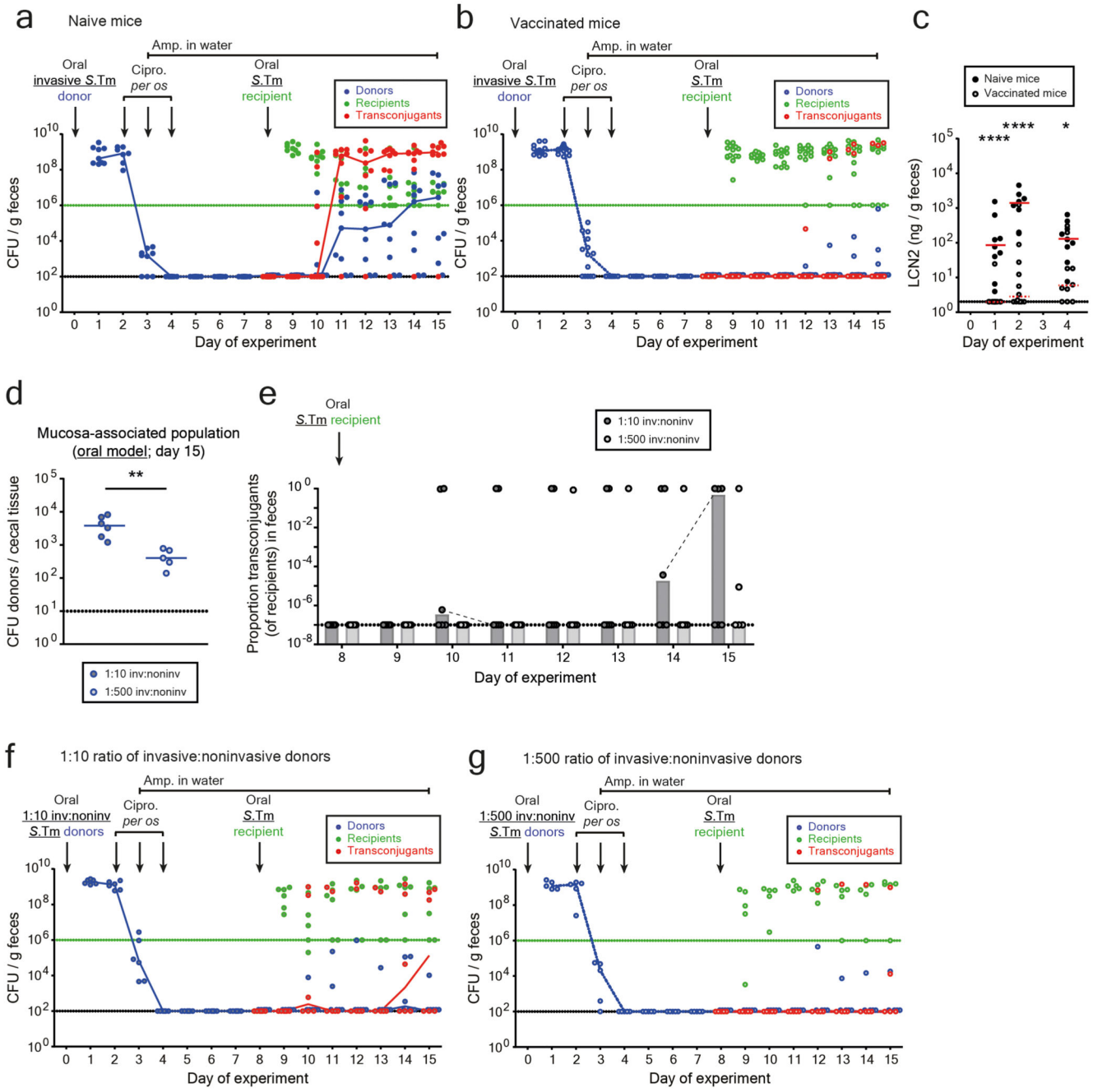

Extended data Fig. 7. Fecal bacterial population sizes and inflammatory status of mice in Figure 3e-f (comparison of vaccinated vs. naïve mice in the oral model) and validation by mixtures of invasive and noninvasive donors.

a-b) Fecal loads of donors (blue; Sm^R, Cm^R), recipients (green; Kan^R), and transconjugants (red; Cm^R, Kan^R) were determined by selective plating on MacConkey agar. Barcode analysis of the recipient chromosome tags could not be performed for technical issues with kanamycin enrichments and subsequent qPCR. Black dotted lines indicate detection limits for donors and transconjugants. Green dotted line indicates detection limit for recipients (the detection limit is higher for recipients once transconjugants reach a density of $>10^8$ CFU/g

feces. Before this happens, recipients can be found below the detection limit and then the black dotted line should be considered as the detection limit). Blue lines connect medians of donor populations; red lines connect medians of transconjugant populations. **a**) Naïve mice infected with invasive *S.*Tm donors (solid circles). **b)** Vaccinated mice infected with invasive *S.*Tm donors (open circles with light-grey fill). **c)** Inflammatory status to determine the success of vaccination was determined by lipocalin-2 ELISA. Statistics are performed using a two-tailed Mann-Whitney U test $p>0.05$ (ns), $p<0.05$ (*), $p<0.01$ (**), $p<0.001$ (***), $p<0.0001$ (****) comparing naïve mice (black circles; n=9 singly housed mice from three independent experiments) to vaccinated mice (open circles; n=14 singly housed mice from four independent experiments) at each time point. Medians are shown (solid red line for naïve mice; dotted red line for vaccinated mice). Dotted line indicates detection limit. **d-g)** Experimentally reducing the population size of mucosa-associated persisters by mixing invasive and noninvasive donors reduces plasmid transfer in the oral model. Mice were orally infected with a mixture of invasive (SL1344 P2^{cat}; Sm^{R}, Cm^{R}) and noninvasive (SL1344^{noninv} P2^{cat}; Sm^{R}, Cm^{R}) donors at two ratios: 1:10 (n=6 singly housed mice) or 1:500 (n=5 singly housed mice). In both cases, an excess of noninvasive donors were used to experimentally reduce the number of cells that can establish a persistent reservoir in the intestinal mucosa (two independent experiments). *S.*Tm 14028S *aphT* (Kan^{R}, Amp^{R}) was used as a recipient after antibiotic treatment. **d)** Donor populations enumerated after a gentamycin protection assay on cecal tissue of mice infected with a 1:10 ratio (blue circles with dark grey fill; line indicates median) or 1:500 ratio (blue circles with light grey fill; line indicates median) of invasive to noninvasive donors. Statistics are performed using a two-tailed Mann-Whitney U test $p<0.01$ (**). **e)** Proportion of transconjugants (transconjugant population size divided by sum of recipients and transconjugants) in the feces is shown for each day for both mice infected with a 1:10 ratio (black circles with dark grey fill; grey bars indicate median) or 1:500 ratio (black circles with light grey fill; light grey bars indicate median) of invasive to noninvasive donors. **f-g)** Fecal loads of donors (blue; Sm^{R}, Cm^{R}), recipients (green; Kan^{R}), and transconjugants (red; Cm^{R}, Kan^{R}) were determined by selective plating on MacConkey agar. **f)** Mice infected with a 1:10 ratio of invasive to noninvasive donors. **g)** Mice infected with a 1:500 ratio of invasive to noninvasive donors. **d-g)** Black dotted line indicates detection limit for donors and transconjugants. Green dotted line indicates detection limit for recipients (the detection limit is higher for recipients once transconjugants reach a density of $>10^{8}$ CFU/g feces. Before this happens, recipients can be found below the detection limit and then the black dotted line should be considered as the detection limit).

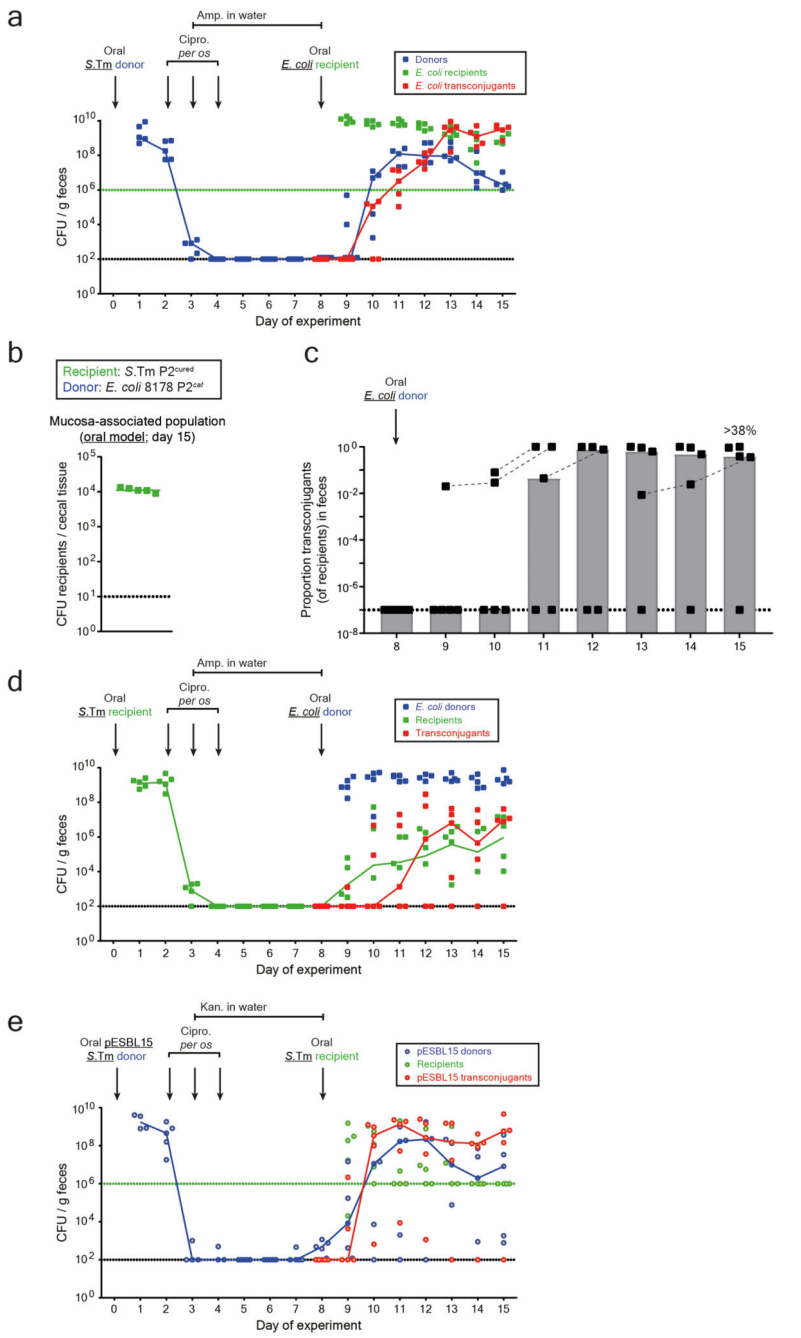

Extended data Fig. 8. Fecal bacterial population sizes of mice in Figure 4 and the role of persistence and conjugation in host tissues if the recipient constitutes the reservoir.

a) Fecal loads of donors (blue; Sm^R, Cm^R), recipients (green; Amp^R), and transconjugants (red; Cm^R, Amp^R) were determined by selective plating on MacConkey agar (same mice as in Fig. 4a-b; *S.*Tm donor and *E. coli* recipient in the oral model). Black dotted line indicates detection limit for donors and transconjugants. Green dotted line indicates detection limit for recipients (the detection limit is higher for recipients once transconjugants reach a density of $>10^8$ CFU/g feces. Before this happens, recipients can be found below the detection limit

and then the black dotted line should be considered as the detection limit). Blue lines connect medians of donor populations; red lines connect medians of transconjugant populations. **b-d)** Persistence in host tissues also promote plasmid transfer if the recipient constitutes the reservoir. Pretreated mice were orally infected with a *S.*Tm recipient (SL1344 $P2^{cured}$ *aphT*; Sm^R, Kan^R) and treated with ciprofloxacin and ampicillin as in the oral model (Fig. 1b). On day 8, ampicillin was removed from the drinking water and an *E. coli* donor was introduced orally (*E. coli* 8178 $P2^{cat}$; Cm^R, Amp^R). **b)** Recipient populations enumerated after a gentamycin protection assay on cecal tissue (n=5 singly housed mice from two independent experiments). Line indicates median. **c)** Proportion of transconjugants (transconjugant population size divided by sum of recipients and transconjugants) in the feces is shown for each day. Grey bars indicate median. **d)** Fecal loads of recipients (green; Sm^R, Kan^R), donors (blue; Cm^R, Amp^R), and transconjugants (red; Sm^R, Cm^R, Kan^R) were determined by selective plating on MacConkey agar. **b-d)** Dotted lines indicate detection limits by selective plating. **e)** Fecal bacterial populations sizes of mice in Figure 4c-d (*S.*Tm ESBL donor in the oral model). Fecal loads of donors (blue; Sm^R, Amp^R), recipients (green; Kan^R), and transconjugants (red; Kan^R, Amp^R) were determined by selective plating on MacConkey agar. Black dotted line indicates detection limit for donors and transconjugants. Green dotted line indicates detection limit for recipients (the detection limit is higher for recipients once transconjugants reach a density of $>10^8$ CFU/g feces. Before this happens, recipients can be found below the detection limit and then the black dotted line should be considered as the detection limit). Blue lines connect medians of donor populations; red lines connect medians of transconjugant populations.

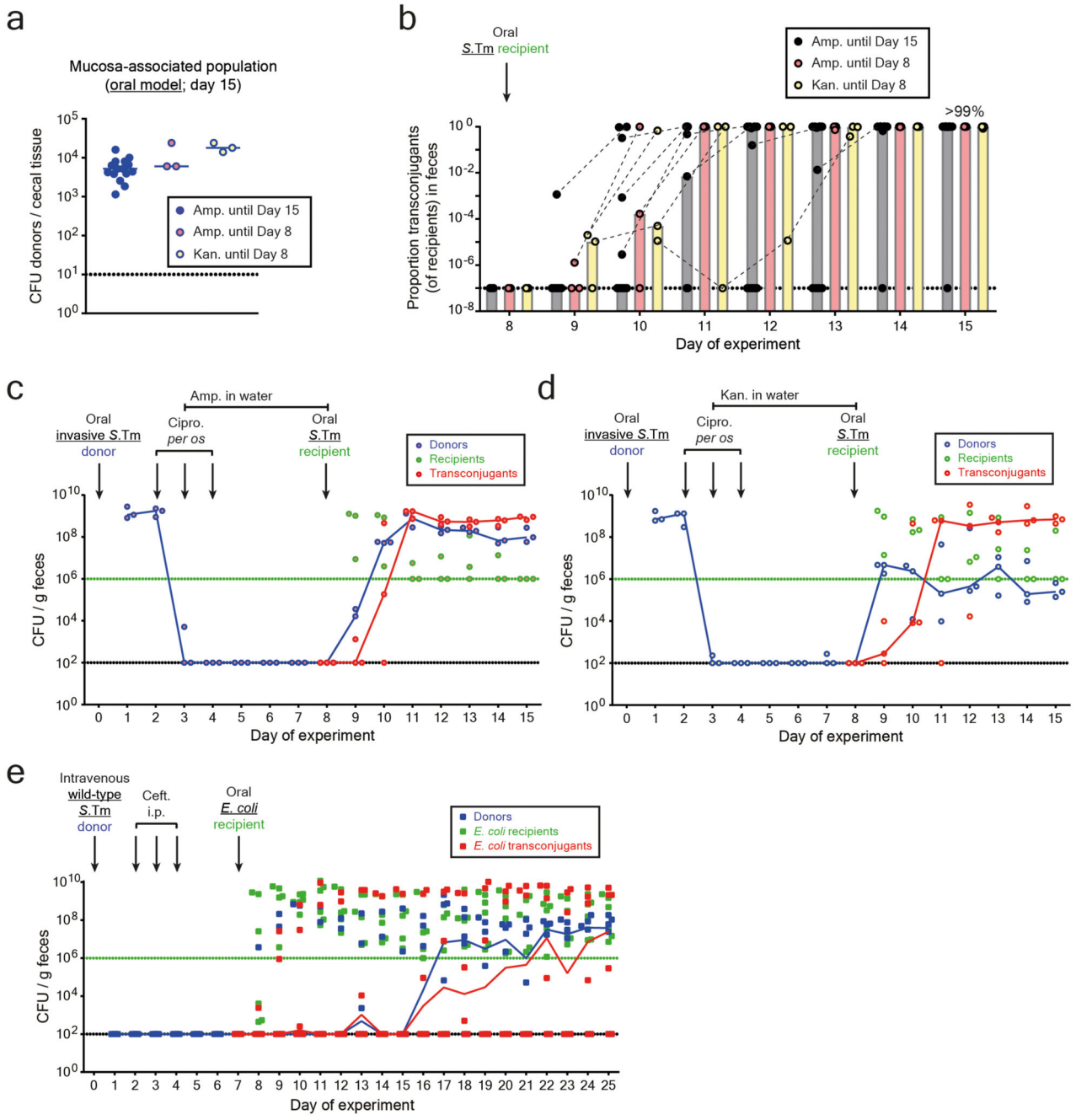

Extended data Fig. 9. Exchanging ampicillin for kanamycin in order to limit gut luminal growth of the donor does not affect the overall plasmid transfer kinetics and fecal bacteria population sizes of I.V. infected mice in Figure 4.

a-d) Mice were orally infected with SL1344 P2^{cat} (Sm^{R}, Cm^{R}) as a donor, and 14028S *aphT* (Kan^{R}, Amp^{R}) as a recipient after antibiotic treatment. Mice were either treated with ampicillin in the drinking water until day 15 (normal protocol as in Fig. 1b), day 8 (when the recipient is added), or kanamycin until day 8. **a)** Donor populations enumerated after a gentamycin protection assay on cecal tissue of mice in which ampicillin is maintained until day 15 (solid blue circles; n=15 singly housed mice from five independent experiments; data

Europe PMC Funders Author Manuscripts

taken from Fig. 1d), ampicillin is removed on day 8 (blue circles with pink fill; n=3 singly housed mice from one experiment), or kanamycin is used until day 8 (blue circles with yellow fill; n=3 singly housed mice from one experiment). Median indicated by solid line. **b)** Proportion of transconjugants (transconjugant population size divided by sum of recipients and transconjugants) is shown for the groups receiving ampicillin treatment until day 15 (solid black circles; grey bars indicate median; n=15 singly housed mice from five independent experiments; data taken from Figure 1c), ampicillin treatment until day 8 (black circles with pink fill; pink bars indicate median; n=3 singly housed mice from one experiment), and kanamycin treatment until day 8 (black circles with yellow fill; yellow bars indicate median; n=3 singly housed mice from one experiment). **c-d)** Fecal loads of donors (blue; Sm^R, Cm^R), recipients (green; Kan^R), and transconjugants (red; Cm^R, Kan^R) were determined by selective plating on MacConkey agar. **c)** Mice treated until day 8 with ampicillin. **d)** Mice treated until day 8 with kanamycin. **a-d)** Black dotted line indicates detection limit for donors and transconjugants. Green dotted line indicates detection limit for recipients (the detection limit is higher for recipients once transconjugants reach a density of $>10^8$ CFU/g feces. Before this happens, recipients can be found below the detection limit and then the black dotted line should be considered as the detection limit). **e)** Fecal bacterial populations sizes of mice in Figure 4E-F (*S.*Tm donor and *E. coli* recipient in the I.V. model). Fecal loads of donors (blue; Sm^R, Amp^R), recipients (green; Kan^R), and transconjugants (red; Kan^R, Amp^R) were determined by selective plating on MacConkey agar. Black dotted line indicates detection limit for donors and transconjugants. Green dotted line indicates detection limit for recipients (the detection limit is higher for recipients once transconjugants reach a density of $>10^8$ CFU/g feces. Before this happens, recipients can be found below the detection limit and then the black dotted line should be considered as the detection limit). Blue lines connect medians of donor populations; red lines connect medians of transconjugant populations.

Europe PMC Funders Author Manuscripts

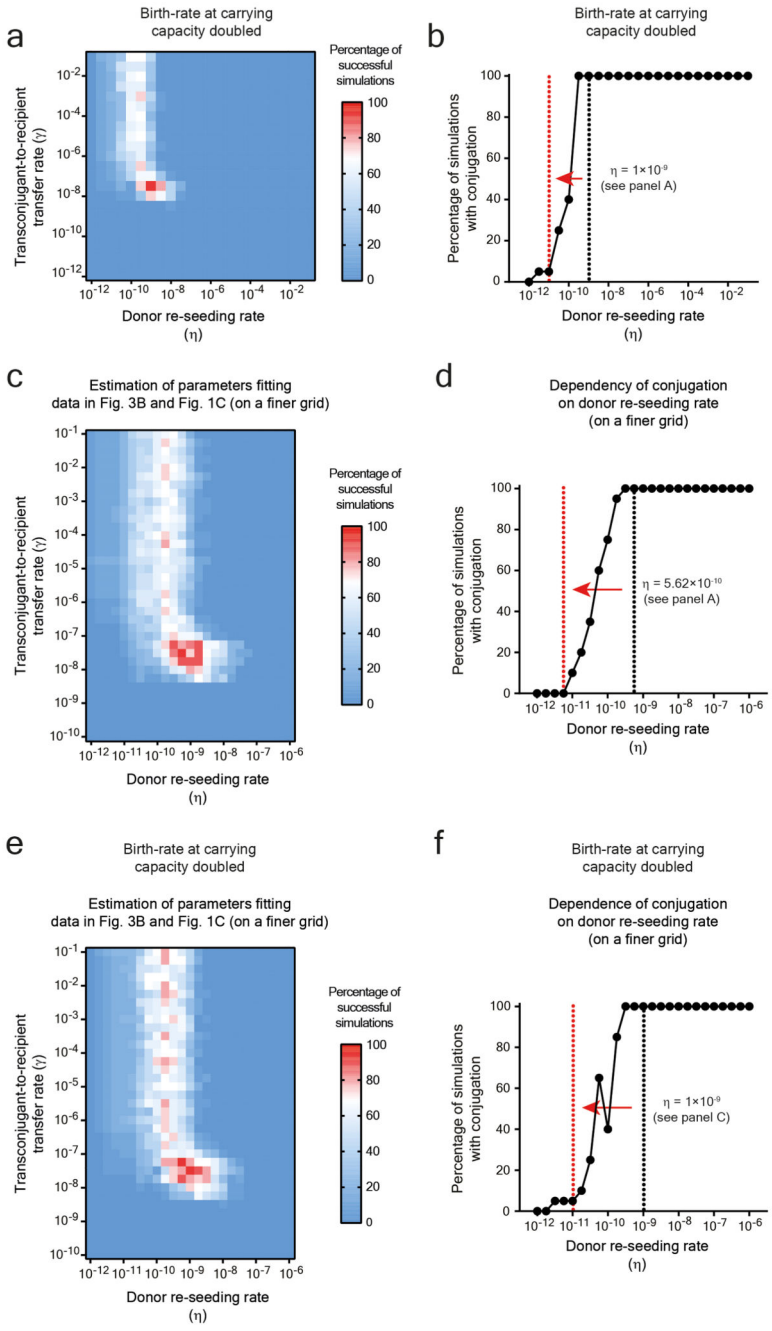

Extended data Fig. 10. Increasing growth rate at carrying capacity to model inflammation or running simulations on a finer parameter grid does not affect overall simulation trends.

a-b) Simulations were run with identical parameters to Figure 3c-d, but an increased birth and death rate at carrying capacity to simulate cases in which inflammation is present (see supplementary material). The trends of the simulations remain the same as in Figure 3c-d. **a)** Likelihood of the model as a function of the donor re-seeding (including donor-to-recipient conjugation) rate (η), and the rate of transconjugant-to-recipient plasmid transfer (γ). All other parameter values are given in the supplementary materials. The most likely parameter

set is shown in red ($\eta = 1\times10^{-9}$ per day; $\gamma = 3.16\times10^{-8}$ per CFU/g feces per day). **b)** The fraction of simulations with plasmid re-seeding, defined as a final transconjugant population size above 5×10^{8} CFU/g feces, as a function of η. Here γ is fixed at its most likely value $\gamma = 3.16\times10^{-8}$ per CFU/g feces per day. The black vertical dotted line at $\eta = 1\times10^{-9}$ per day indicates the estimated most likely value (from **panel a**). The red vertical dotted line at $\eta = 1\times10^{-11}$ per day indicates a hypothetical 100-fold decrease of η (shown by a red arrow; e.g. by vaccination). **c-f)** Running simulations on a finer parameter grid does not affect overall simulation trends. See Supplementary table 4 for details on differences between specific simulation results. **c-d)** Simulations were run on a grid of [$\eta = 10^{-12}$-10^{-6}, $\gamma = 10^{-10}$-10^{-1}] with 0.25 log increments (rather than the [$\eta = 10^{-12}$-10^{-1}, $\gamma = 10^{-12}$-10^{-1}] with 0.5 log increments used in Figure 3c-d). **e-f)** Simulations were run with parameters identical to **panel a-b**, but on a grid of [$\eta = 10^{-12}$-10^{-6}, $\gamma = 10^{-10}$-10^{-1}] with 0.25 log increments (rather than the [$\eta = 10^{-12}$-10^{-1}, $\gamma = 10^{-12}$-10^{-1}] with 0.5 log increments). **c, e)** Likelihood of the model as a function of the donor re-seeding (including donor-to-recipient conjugation) rate (η), and the rate of transconjugant-to-recipient plasmid transfer (γ). All other parameter values are given in the supplementary materials. The most likely parameter set is shown in red. **d, f)** The fraction of simulations with plasmid re-seeding, defined as a final transconjugant population size above 5×10^{8} CFU/g feces, as a function of η. Here γ is fixed at its most likely value. The black vertical dotted line indicates the estimated most likely value (from **panel c or e**). The red vertical dotted line indicates a hypothetical 100-fold decrease of η (shown by a red arrow; e.g. by vaccination).

Supplementary Material

Refer to Web version on PubMed Central for supplementary material.

Acknowledgements

We would like to extend our gratitude to the members of the Hardt, Slack, Bonhoeffer, Stadler, and Ackermann labs for helpful discussion, and to the staff at the RCHCI and EPIC animal facilities for their excellent support. This work has been funded in part by grants from the Swiss National Science Foundation (SNF; 310030B-173338), the Promedica Foundation, Chur and the Helmut Horten Foundation to WDH, and from the SNF (407240-167121) to WDH, SB, and AE. MD is funded by an SNF professorship grant (PP00PP_176954), EB by a Boehringer Ingelheim Fonds PhD fellowship, and MES and partly SAF by the Swedish Research Council (2015-00635, 2018-02223). RRR is funded by SNF grant number 31003A_149769. ES is supported by grant GRS 073/17 from the"Microbials" programme of the Gebert Rüf Foundation and the SNF Bridge Discover Grant 20B2-1 180953. The authors declare no conflict of interest, financial or otherwise.

References

1. Parisi A, et al. Health Outcomes from Multidrug-Resistant Salmonella Infections in High-Income Countries: A Systematic Review and Meta-Analysis. Foodborne Pathog Dis. 2018; doi: 10.1089/fpd.2017.2403
2. Wright GD. The antibiotic resistome: the nexus of chemical and genetic diversity. Nat Rev Microbiol. 2007; 5:175–186. DOI: 10.1038/nrmicro1614 [PubMed: 17277795]
3. Brauner A, Fridman O, Gefen O, Balaban NQ. Distinguishing between resistance, tolerance and persistence to antibiotic treatment. Nat Rev Microbiol. 2016; 14:320–330. DOI: 10.1038/nrmicro.2016.34 [PubMed: 27080241]
4. Fridman O, Goldberg A, Ronin I, Shoresh N, Balaban NQ. Optimization of lag time underlies antibiotic tolerance in evolved bacterial populations. Nature. 2014; 513:418–421. DOI: 10.1038/nature13469 [PubMed: 25043002]

5. Claudi B, et al. Phenotypic variation of *Salmonella* in host tissues delays eradication by antimicrobial chemotherapy. Cell. 2014; 158:722–733. DOI: 10.1016/j.cell.2014.06.045 [PubMed: 25126781]
6. Helaine S, et al. Internalization of Salmonella by macrophages induces formation of nonreplicating persisters. Science. 2014; 343:204–208. DOI: 10.1126/science.1244705 [PubMed: 24408438]
7. Kaiser P, et al. Cecum lymph node dendritic cells harbor slow-growing bacteria phenotypically tolerant to antibiotic treatment. PLoS Biol. 2014; 12:e1001793.doi: 10.1371/journal.pbio.1001793 [PubMed: 24558351]
8. Dolowschiak T, et al. IFN-gamma Hinders Recovery from Mucosal Inflammation during Antibiotic Therapy for Salmonella Gut Infection. Cell Host Microbe. 2016; 20:238–249. DOI: 10.1016/j.chom.2016.06.008 [PubMed: 27453483]
9. Balaban NQ, et al. Definitions and guidelines for research on antibiotic persistence. Nat Rev Microbiol. 2019; doi: 10.1038/s41579-019-0196-3
10. Balaban NQ, Merrin J, Chait R, Kowalik L, Leibler S. Bacterial persistence as a phenotypic switch. Science. 2004; 305:1622–1625. DOI: 10.1126/science.1099390 [PubMed: 15308767]
11. Levin-Reisman I, et al. Antibiotic tolerance facilitates the evolution of resistance. Science. 2017; 355:826–830. DOI: 10.1126/science.aaj2191 [PubMed: 28183996]
12. Wotzka SY, et al. Microbiota stability in healthy individuals after single-dose lactulose challenge-A randomized controlled study. PLoS One. 2018; 13:e0206214.doi: 10.1371/journal.pone.0206214 [PubMed: 30359438]
13. Coque TM, Baquero F, Canton R. Increasing prevalence of ESBL-producing Enterobacteriaceae in Europe. Euro Surveill. 2008; 13
14. Crump JA, Sjolund-Karlsson M, Gordon MA, Parry CM. Epidemiology, Clinical Presentation, Laboratory Diagnosis, Antimicrobial Resistance, and Antimicrobial Management of Invasive Salmonella Infections. Clin Microbiol Rev. 2015; 28:901–937. DOI: 10.1128/CMR.00002-15 [PubMed: 26180063]
15. Wilcock BP, Armstrong CH, Olander HJ. The significance of the serotype in the clinical and pathological features of naturally occurring porcine salmonellosis. Can J Comp Med. 1976; 40:80–88. [PubMed: 793690]
16. Wood RL, Pospischil A, Rose R. Distribution of persistent Salmonella typhimurium infection in internal organs of swine. Am J Vet Res. 1989; 50:1015–1021. [PubMed: 2528309]
17. San Roman B, et al. Relationship between Salmonella infection, shedding and serology in fattening pigs in low-moderate prevalence areas. Zoonoses Public Health. 2018; doi: 10.1111/zph.12453
18. Tenaillon O, Skurnik D, Picard B, Denamur E. The population genetics of commensal Escherichia coli. Nat Rev Microbiol. 2010; 8:207–217. DOI: 10.1038/nrmicro2298 [PubMed: 20157339]
19. Apperloo-Renkema HZ, Van der Waaij BD, Van der Waaij D. Determination of colonization resistance of the digestive tract by biotyping of Enterobacteriaceae. Epidemiol Infect. 1990; 105:355–361. DOI: 10.1017/s0950268800047944 [PubMed: 2209739]
20. Stecher B, et al. Gut inflammation can boost horizontal gene transfer between pathogenic and commensal Enterobacteriaceae. Proc Natl Acad Sci U S A. 2012; 109:1269–1274. DOI: 10.1073/pnas.1113246109 [PubMed: 22232693]
21. Diard M, et al. Inflammation boosts bacteriophage transfer between Salmonella spp. Science. 2017; 355:1211–1215. DOI: 10.1126/science.aaf8451 [PubMed: 28302859]
22. Moor K, et al. High-avidity IgA protects the intestine by enchaining growing bacteria. Nature. 2017; doi: 10.1038/nature22058
23. Monack DM, Bouley DM, Falkow S. Salmonella typhimurium persists within macrophages in the mesenteric lymph nodes of chronically infected Nramp1+/+ mice and can be reactivated by IFNgamma neutralization. J Exp Med. 2004; 199:231–241. DOI: 10.1084/jem.20031319 [PubMed: 14734525]
24. Diard M, et al. Antibiotic treatment selects for cooperative virulence of Salmonella typhimurium. Curr Biol. 2014; 24:2000–2005. DOI: 10.1016/j.cub.2014.07.028 [PubMed: 25131673]
25. Sampei G, et al. Complete genome sequence of the incompatibility group I1 plasmid R64. Plasmid. 2010; 64:92–103. DOI: 10.1016/j.plasmid.2010.05.005 [PubMed: 20594994]

26. Hensel M, et al. Simultaneous identification of bacterial virulence genes by negative selection. Science. 1995; 269:400–403. [PubMed: 7618105]
27. Stapels DAC, et al. Salmonella persisters undermine host immune defenses during antibiotic treatment. Science. 2018; 362:1156–1160. DOI: 10.1126/science.aat7148 [PubMed: 30523110]
28. Moor K, et al. Peracetic Acid Treatment Generates Potent Inactivated Oral Vaccines from a Broad Range of Culturable Bacterial Species. Front Immunol. 2016; 7:34.doi: 10.3389/fimmu.2016.00034 [PubMed: 26904024]
29. Fauvart M, De Groote VN, Michiels J. Role of persister cells in chronic infections: clinical relevance and perspectives on anti-persister therapies. J Med Microbiol. 2011; 60:699–709. DOI: 10.1099/jmm.0.030932-0 [PubMed: 21459912]
30. Roberts ME, Stewart PS. Modelling protection from antimicrobial agents in biofilms through the formation of persister cells. Microbiology. 2005; 151:75–80. DOI: 10.1099/mic.0.27385-0 [PubMed: 15632427]
31. Knodler LA, et al. Noncanonical inflammasome activation of caspase-4/caspase-11 mediates epithelial defenses against enteric bacterial pathogens. Cell Host Microbe. 2014; 16:249–256. DOI: 10.1016/j.chom.2014.07.002 [PubMed: 25121752]
32. Sellin ME, et al. Epithelium-intrinsic NAIP/NLRC4 inflammasome drives infected enterocyte expulsion to restrict *Salmonella* replication in the intestinal mucosa. Cell Host Microbe. 2014; 16:237–248. DOI: 10.1016/j.chom.2014.07.001 [PubMed: 25121751]
33. Defraine V, Fauvart M, Michiels J. Fighting bacterial persistence: Current and emerging anti-persister strategies and therapeutics. Drug Resist Updat. 2018; 38:12–26. DOI: 10.1016/j.drup.2018.03.002 [PubMed: 29857815]
34. Grant AJ, et al. Modelling within-host spatiotemporal dynamics of invasive bacterial disease. PLoS Biol. 2008; 6:e74.doi: 10.1371/journal.pbio.0060074 [PubMed: 18399718]
35. Datsenko KA, Wanner BL. One-step inactivation of chromosomal genes in Escherichia coli K-12 using PCR products. Proc Natl Acad Sci U S A. 2000; 97:6640–6645. DOI: 10.1073/pnas.120163297 [PubMed: 10829079]
36. Sternberg NL, Maurer R. Bacteriophage-mediated generalized transduction in Escherichia coli and Salmonella typhimurium. Methods Enzymol. 1991; 204:18–43. [PubMed: 1943777]
37. Stecher B, et al. Chronic Salmonella enterica serovar Typhimurium-induced colitis and cholangitis in streptomycin-pretreated Nramp1+/+ mice. Infect Immun. 2006; 74:5047–5057. DOI: 10.1128/IAI.00072-06 [PubMed: 16926396]
38. Barthel M, et al. Pretreatment of mice with streptomycin provides a Salmonella enterica serovar Typhimurium colitis model that allows analysis of both pathogen and host. Infect Immun. 2003; 71:2839–2858. [PubMed: 12704158]
39. Johansson ME, Hansson GC. Preservation of mucus in histological sections, immunostaining of mucins in fixed tissue, and localization of bacteria with FISH. Methods Mol Biol. 2012; 842:229–235. DOI: 10.1007/978-1-61779-513-8_13 [PubMed: 22259139]
40. Marjoram P, Molitor J, Plagnol V, Tavare S. Markov chain Monte Carlo without likelihoods. Proc Natl Acad Sci U S A. 2003; 100:15324–15328. DOI: 10.1073/pnas.0306899100 [PubMed: 14663152]
41. Zankari E, et al. Identification of acquired antimicrobial resistance genes. J Antimicrob Chemother. 2012; 67:2640–2644. DOI: 10.1093/jac/dks261 [PubMed: 22782487]

Europe PMC Funders Author Manuscripts

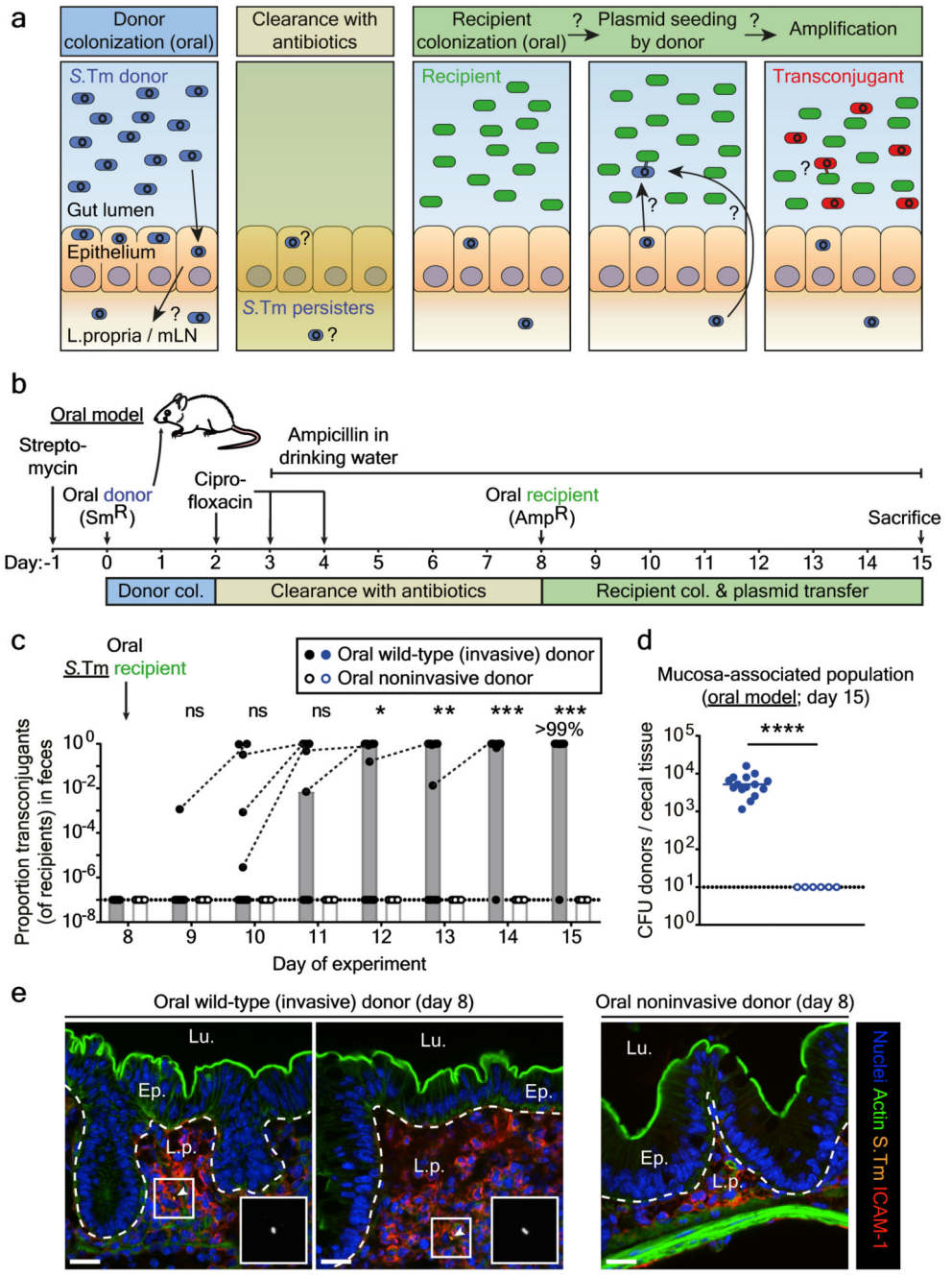

Figure 1. Gut-tissue associated *S.*Tm persisters are a reservoir for conjugative plasmids.

a) Working hypothesis. Plasmid-bearing *S.*Tm (blue) form persisters (smaller, circular shape) in gut tissues and the mLN. These can survive antibiotic treatment, re-seed the gut lumen and transfer their plasmid to recipients (green). Transconjugants (red) can further amplify plasmid spread. **b)** Oral infection mouse model. **c)** Donor mucosa invasion is required for persister-promoted plasmid transfer. Invasive (SL1344 P2^{cat}; Sm^R, Cm^R) or non-invasive *S.*Tm (SL1344^{noninv} P2^{cat}; TTSS-1 negative; Sm^R, Cm^R) were used as donors and *S.*Tm 14028S *aphT* (P2 free) as recipients (Kan^R, Amp^R), as shown in **panel b**.

Transconjugant proportions in feces from experiments with invasive (solid black circles; grey bars indicate median; n=15 mice; 5 independent experiments; n=9 mice pooled from data in Fig. 3) or noninvasive donors (open black circles; white bars indicate median; n=6 mice; 2 independent experiments). Dashed lines connect data points from the same mice. **d)** Donor reservoirs in the cecal mucosa from mice as infected in **panel c** were quantified by tissue gentamycin protection. Solid blue circles: invasive donors; open blue circles: noninvasive donors; lines indicate the median; Statistics are performed using a two-tailed Mann-Whitney U test ($p>0.05$ (ns), $p<0.05$ (*), $p<0.01$ (**), $p<0.001$ (***), $p<0.0001$ (****)). Dotted line: detection limit. **e)** Persisters in the cecum lamina propria (oral model; day 8). *S.*Tm (yellow; α-LPS O5 and α-LPS O12 staining), nuclei (blue), actin (green) and lamina propria (ICAM-1; red) are stained. Ep., epithelium; Lu., Lumen; L.p., lamina propria. Scale bars=20μm. White arrows highlight *S.*Tm (magnified in inset). Representative of three independent experiments. Quantification is provided in Extended Data Fig. 4.

Europe PMC Funders Author Manuscripts

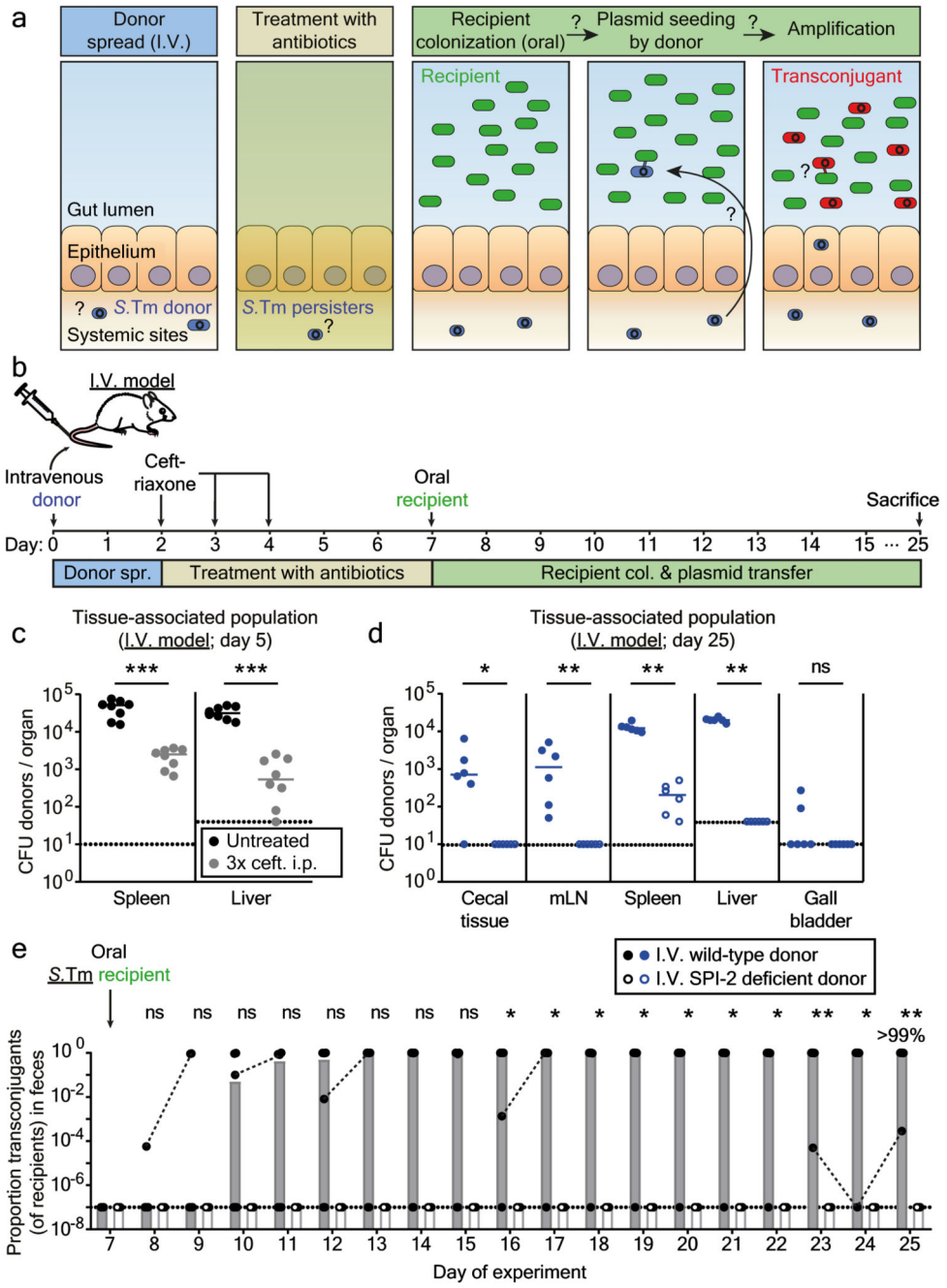

Figure 2. Persisters at systemic sites are a reservoir for plasmid transfer in the gut.

a) Working hypothesis. Same as Fig. 1a, but donors are introduced by intravenous infection. **b)** I.V. infection mouse model. **c)** Persisters in the spleens and livers. In two independent experiments, n=8 mice (grey circles) were infected i.v. with an equal mix of five SL1344 P2*cat TAG* strains (Sm^R, Cm^R). Black circles indicate control mice (n=8) infected for 5 days without ceftriaxone treatment. Extended Data Fig. 5a shows counts for additional organs. **d-e)** SPI-2 promotes donor reservoir formation at systemic sites. In two independent experiments, mice were infected as described in panel B with donors, i.e. mixtures of five

Europe PMC Funders Author Manuscripts

wild-type (n=6; closed circles) or SPI-2 deficient (n=6; open circles) SL1344 P2*cat TAG* strains (Sm^R, Cm^R). **d)** Donor populations in internal organs from mice infected with wild-type (solid blue) or SPI-2 deficient donors (open blue). Lines indicate the median. **e)** Fecal populations from mice from **panel d**. Transconjugant proportions in feces from experiments with wild-type (solid black circles; grey bars indicate median) or noninvasive donors (open black circles; white bars indicate median). Dashed lines connect data points from the same mice. Statistics are performed using a two-tailed Mann-Whitney U test ($p>0.05$ (ns), $p<0.05$ (*), $p<0.01$ (**), $p<0.001$ (***)). Dotted lines: detection limits.

Europe PMC Funders Author Manuscripts

Europe PMC Funders Author Manuscripts

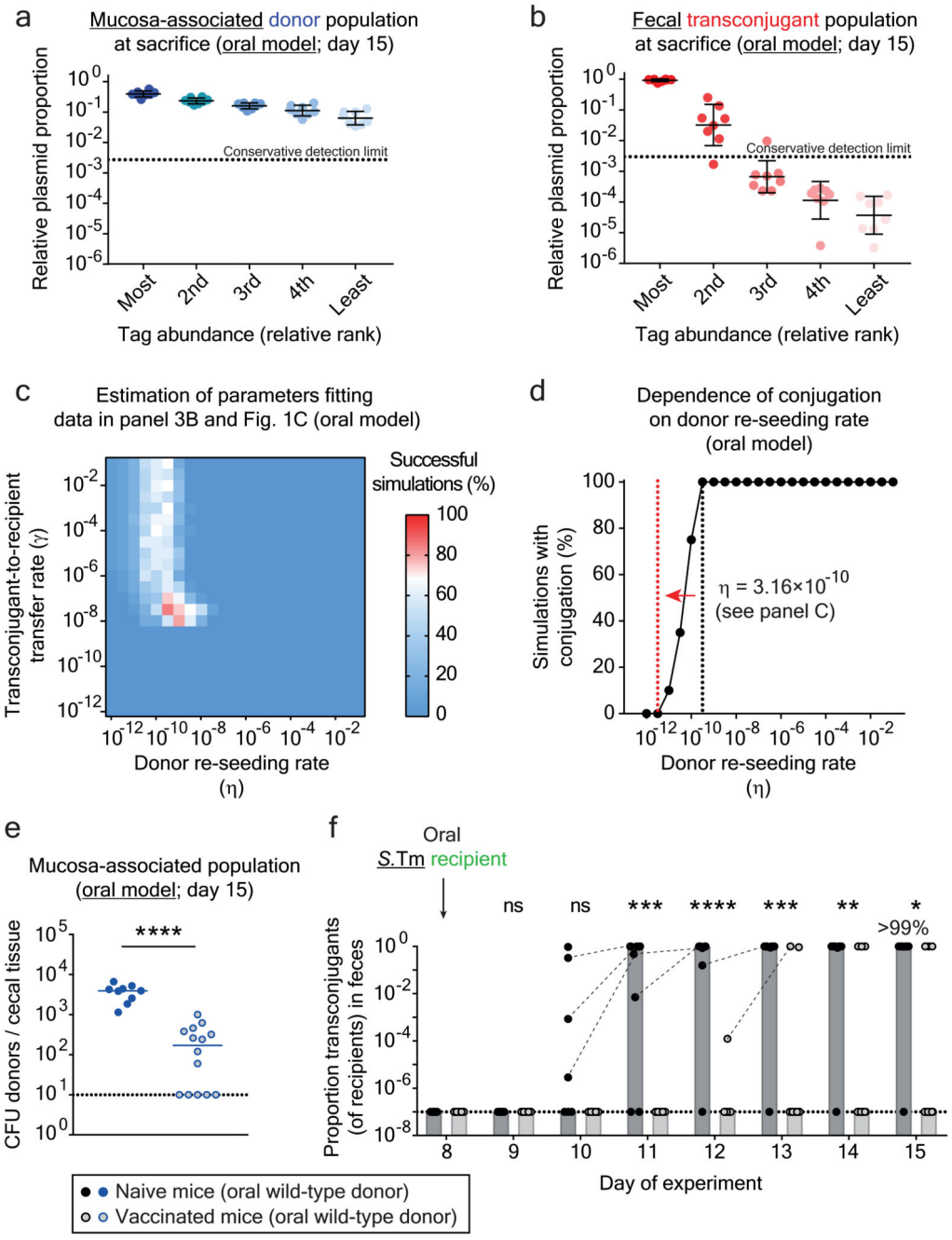

Figure 3. Plasmid transfer is initiated by rare donor re-seeding events and can be prevented by vaccination.

Mice were orally infected (Fig. 1b) with tagged donor (five SL1344 P2$^{cat\ TAG}$; Sm^{R}, Cm^{R}) and recipient mixtures (five 14028S *TAG* strains; Kan^{R}, Amp^{R}; n=8 mice; three independent experiments). Donors, recipients and transconjugants were enumerated by plating (Extended Data Fig. 7a) and plasmid-tag distributions analyzed by qPCR (raw data shown in Extended Data Fig. 6b). **a-b)** Plasmid-tag distribution in mucosa-associated donors and fecal transconjugants at day 15. Dotted lines indicate conservative qPCR detection limits

(2.9×10^{-3}). Line indicates mean; error bars indicate standard deviation. **c)** Modeling results. Simulations are described in the supplementary discussion. A rate of donor re-seeding and donor-to-recipient conjugation of $\eta = 3.16\times10^{-10}$ per day and a rate of transconjugant-to-recipient conjugation of $\gamma = 3.16\times10^{-8}$ per CFU/g feces per day optimally fit the data (red). **d)** Effect of η on transconjugant detection. Analysis as described in the supplementary discussion. Reducing η by 100-fold below the value estimated for naïve mice (black dotted line; $\eta = 3.16\times10^{-10}$) diminishes transconjugant detection (red dotted line). **e-f)** Vaccination diminishes conjugation. Mice vaccinated with killed *S.*Tm (open circles; n = 14; four independent experiments) or PBS (naïve; closed circles; n = 9; three independent experiments) were infected with tagged donor and recipient mixtures as in **panel a-b**. Donors, recipients and transconjugants were enumerated by plating. **e)** Mucosa-associated donor populations at day 15. **f)** Fecal transconjugant proportions in naive (black circles; grey bars indicate median) or vaccinated mice (light gray circles; light gray bars indicate median) from **panel e**. Dashed lines connect data points from the same mice. Statistics are performed using a two-tailed Mann-Whitney U test ($p>0.05$ (ns), $p<0.05$ (*), $p<0.01$ (**), $p<0.001$ (***), $p<0.0001$ (****)). Dotted lines: detection limits.

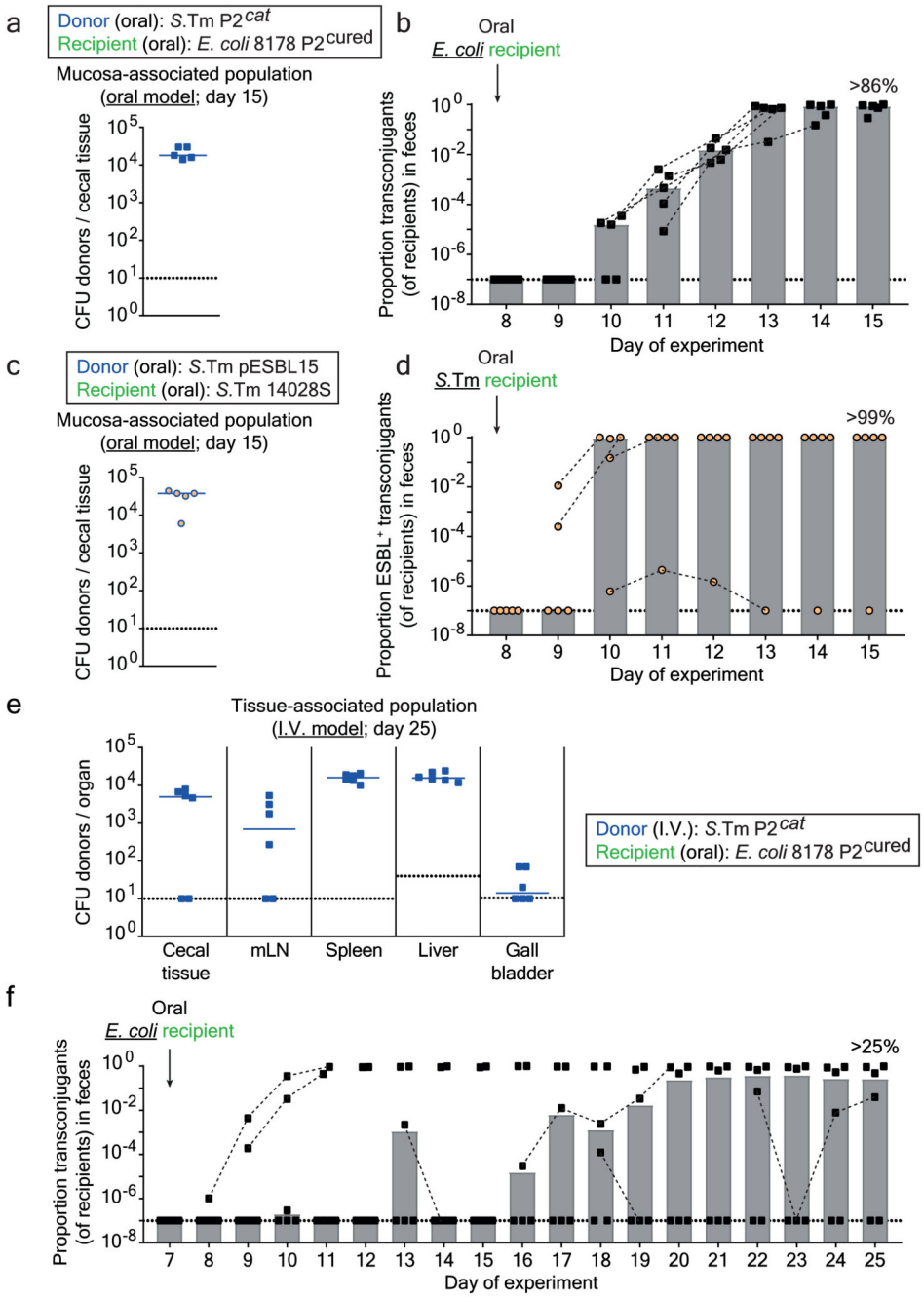

Figure 4. Tissue-associated persisters promote resistance plasmid transfer between different Enterobacteriaceae.

a-b) Plasmid transfer to *E. coli*. 5 mice (one experiment) were infected orally as described in Fig. 1b-d with donors (*S.*Tm SL1344 P2^{cat}; Sm^{R}, Cm^{R}) and recipients (*E. coli* 8178 P2^{cured} (Amp^{R})). Mucosa-associated donors and fecal transconjugants were enumerated by plating. Median indicated by solid line. Bars indicate median. **c-d)** ESBL plasmid transfer between *Salmonella* spp.. The experiment used *S.*Tm SL1344 pESBL15; Sm^{R}, Amp^{R} as the donor and *S.*Tm 14028S *aphT*; Kan^{R} as recipient (n=5 mice; one experiment). It was performed

and evaluated as in **panels a-b**, except that we used kanamycin from day 3-8 instead of ampicillin in the drinking water, since pESBL15 confers ampicillin resistance. **e-f)** Plasmid transfer from *S.*Tm to *E. coli* using the i.v. model. 6 mice (two independent experiments) were infected as described in Fig. 2b-e with donors (*S.*Tm SL1344 P2^{cat}; Sm^{R}, Cm^{R}; i.v.) and recipients (*E. coli* 8178 P2^{cured} (Amp^{R}); oral). Tissue-associated donors and fecal transconjugants were enumerated by plating. Median indicated by solid line. Bars indicate median. **Panel a-f)** Dotted lines indicate detection limit by selective plating. **Panel b, d, f)** Dashed lines connect data points from the same mice to illustrate the progression of plasmid spread after initial detection.

Europe PMC Funders Author Manuscripts